

The SIS process on Erdős-Rényi graphs: determining the infected fraction

O.S. Awolude¹, E. Cator¹, and H. Don¹

¹*Department of Mathematics, Radboud University, Heyendaalseweg 135, Nijmegen, 6525 AJ, Gelderland, Netherlands*

November 18, 2024

Abstract

There are many methods to estimate the quasi-stationary infected fraction of the SIS process on (random) graphs. A challenge is to adequately incorporate correlations, which is especially important in sparse graphs. Methods typically are either significantly biased in sparse graphs, or computationally very demanding already for small network sizes. The former applies to Heterogeneous Mean Field and to the N -intertwined Mean Field Approximation, the latter to most higher order approximations.

In this paper we present a new method to determine the infected fraction in sparse graphs, which we test on Erdős-Rényi graphs. Our method is based on degree-pairs, does take into account correlations and gives accurate estimates. At the same time, computations are very feasible and can easily be done even for large networks.

Keywords: SIS Process, Sparse Graphs, Erdős-Rényi Graph, Metastable Behaviour, Infected Fraction

1 Introduction

The Covid-19 virus was first identified in Wuhan (China) in December 2019, when it started to spread very quickly worldwide. In this initial stage, the number of cases was growing exponentially fast and the disease was disrupting society. In the next few years, many people got infected and there were several peaks of infections of the virus and its variants. Right now, it seems the situation is stabilizing. A large part of the world population has been infected at least once and many people have built up immunity. The number of new cases has dropped, but the disease still goes around and is expected to stay forever. The World Health Organization (WHO) shifts its focus from emergency response to long term Covid-19 disease management [32]. In this paper, we show how to estimate and explain the behaviour of infectious diseases after stabilization.

Mathematical models for infectious diseases have been studied over the last decades, with a recently boosted interest due to the Covid-19 outbreak. In this work we focus on the Markovian SIS process (contact process in the mathematical literature) on finite graphs. In this model, individuals are represented by nodes in a graph, which are either healthy or infected. Each infected node heals at rate 1, and it infects each of its healthy neighbors at rate τ . This means that healthy individuals are always susceptible to the disease, like in the endemic Covid-19 phase. It motivates the terminology susceptible-infected-susceptible (SIS). For more background on the SIS process and related models, we refer to [27, 24, 10, 22].

The SIS process was first introduced by Harris [18] in 1974. Harris studied the process on the integer lattice \mathbb{Z}^d . It has later been studied on many other graphs [23, 28, 8, 36, 39], with recent attention to the process on random graphs [4, 6, 20, 29, 30]. Random graphs are designed to model social connections within populations, and as such are suitable to model a population in which an infectious disease is spreading. Our focus in this paper is on the SIS process on Erdős-Rényi random graphs [13, 16]. For background on random graphs in general and the Erdős-Rényi graph in particular, we refer to [14, 5, 41].

A key characteristic of the SIS model on the Erdős-Rényi graph (and many other graphs) is the existence of an epidemic threshold. Below this threshold, the infection dies out exponentially fast. Above the epidemic threshold, extinction only happens at a very large time scale, see [6, 12, 15]. On finite graphs, ultimately the process will reach the only stable solution in which all individuals are healthy. However, before extinction, the process will be in a *metastable* or *quasi-stationary* state, which is quickly reached [19] and corresponds to the Covid-19 endemic phase. Our primary goal in this paper is to get a better understanding of this stabilized behaviour of the SIS-process on sparse graphs, for which the Erdős-Rényi graph is our main test case. We are particularly aiming at determining the infected fraction of the population in the metastable state based on the parameters of the process and on graph characteristics.

1.1 Review of models for the infected fraction

Exact analysis of the SIS process and its metastable state is hard, and only few rigorous results are available, even for quite simple graphs [8]. For a general graph given by its adjacency matrix, the probability distribution on the state space can in principle be computed numerically at any time. However, due to the exponential size of the state space, these matrix computations are limited to very small populations.

This is the reason that a lot of attention has gone to methods for approximating the behaviour of the process, see [34, 22] for a discussion of some different approaches. Kephart and White consider the process on regular graphs, and derive a differential equation for the evolution of the infected fraction [21]. Wang et al. [44] had the interesting idea to generalize this to graphs with arbitrary adjacency matrix, but their results were shown to be inaccurate in the metastable regime [43]. This inspired Van Mieghem et al. [43] to introduce the N -intertwined Mean Field Approximation (NIMFA), which requires solving a system with ‘only’ n unknowns to approximate the metastable infected fraction (n being the population size). As the authors note, NIMFA overestimates the metastable infected fraction because it ignores correlations between nodes. This is especially problematic if degrees in the graph are small.

The Heterogeneous Mean Field approximation (HMF) in [35] also ignores correlations. In fact, for graphs with exponentially decaying degree distributions (like the Erdős-Rényi graph), [35] proposes to ignore fluctuations in the degree and just use the average. This is the *homogeneous* mean field approximation. Although this is reasonable if the degrees are not too small, it leads to inaccurate estimates for sparse Erdős-Rényi graphs. HMF is proposed in [35] for scale-free graphs, i.e. graphs in which the degree distribution decays polynomially. HMF is a degree-based mean field approach (DBMF), which can also be used for sparse Erdős-Rényi graphs. Also HMF suffers from overestimation because correlations are ignored.

NIMFA is also known as the individual-based mean field approach (IBMF). There are several ways to include higher order terms and extend this to a pair-based mean field approach (PBMF), also known as pair-quenched mean field (PQMF), see for instance [7, 26, 37, 38]. These methods have improved accuracy at the cost of more computations. In some cases the solutions might be unstable and physically meaningless [7]. Another approach is to use the master equation given in [17]. This is computationally very demanding, even for small networks. In practice, one has to use approximate forms. The cavity master equation (CME) [2] gives an alternative system of coupled differential equations, based on conditional probabilities rather than expectations of products. In its full form, it is again challenging to solve. By degree-based averaging, the system can be reduced to a feasible size, coined CME-1 in [33]. This greatly simplifies the calculations and is quite promising, although the system is not closed and can not be solved without a suitable Ansatz. Higher order CME approximations take a larger neighborhood of each node into account [25]. Also here, assumptions to close the system are needed. See [33] for a more detailed comparison of the different higher order methods. In summary, there is always a trade-off between the level of accuracy and the feasibility of computations.

Our main results are listed in Sec. 2.4, after the definitions in 2.1, a comparison with the complete graph in 2.2, and a discussion on annealed and quenched estimation in 2.3. When degrees in the graph are small, it is important to take the degree distribution and correlations between nodes into account. Section 3 builds the framework for all our heuristics. Both NIMFA and HMF fit into this framework. Section 4 demonstrates how to include correlations, and discusses asymptotics when the degrees go to infinity. Section 5 presents the numerical results. This includes a discussion on subcritical disconnected Erdős-Rényi graphs. We also show how our methods can be used to estimate correlations and individual infection probabilities. The methods are suitable to be applied beyond Erdős-Rényi graphs.

2 Preliminaries and goals

2.1 Model definitions

The goal of this paper is to predict and understand the behaviour of the SIS process on Erdős-Rényi graphs. In particular we are interested in the quasi-stationary behaviour. Which fraction of the population will be infected on average if the process has reached its metastable equilibrium?

We denote the set of nodes in our Erdős-Rényi graph by $V = \{1, 2, \dots, n\}$. Each pair of nodes $\{i, j\}$ is connected (notation: $i \sim j$) with probability p , independent of all other pairs. This random graph is denoted $G_{n,p}$. The same notation and terminology will be used for realizations of the random graph as well. We typically take p to be a decreasing function of n . For instance, if $p = c/n$ for some constant c , the average degree does not depend on the size of the population. In this case c has to be greater than 1, otherwise the graph only has small components which do not interact. If $c > 1$, there is a unique *giant* component, containing a positive fraction of the population also for $n \rightarrow \infty$. The graph then is called supercritical. All Erdős-Rényi graphs in this paper are assumed to satisfy this criterion. Another threshold is $p = \log(n)/n$, when (almost) all nodes are in the giant component.

On such an Erdős-Rényi graph $G = (V, E)$, we define our Markovian SIS process. This process is a continuous-time process, with state space 2^V . The state represents the set of infected nodes. Suppose $I \subseteq V$ is the set of infected nodes. The transition rates are then defined by

$$\begin{aligned} I &\rightarrow I \setminus \{i\} \text{ with rate } \delta, & i &\in I, \\ I &\rightarrow I \cup \{j\} \text{ with rate } \#\{i \in I : i \sim j\} \cdot \tau, & j &\in V \setminus I. \end{aligned}$$

The healing rate for each infected node is δ . Throughout this paper, we will stick to the convention that $\delta = 1$, without loss of generality. The infection rate of an infected node to each of its healthy neighbors is τ . Also for τ , we will often take a function of n .

For each node i , we let $X_i(t)$ denote the status of node i at time t , where $X_i(t)$ is either 1 (infected) or 0 (healthy). The total number of infected nodes at time t is denoted by $X(t)$. Furthermore, we let

$$\bar{X}(t) = \frac{1}{n} \sum_{i=1}^n X_i(t) = \frac{X(t)}{n}$$

denote the infected fraction of the population at time t . Quasi-stationarity means that the probability distribution of these quantities is (almost) independent of t in a large time window. Such behaviour will happen if the parameters admit a non-trivial state where healings and infections are balanced. For the complete graph, it is known that the quasi-stationary distribution is a well-defined object. This requires taking limits of n and t in the right way, see [3]. Similar behaviour is observed to appear in other graphs, in particular Erdős-Rényi graphs. Figure 1 clearly shows that the number of infected individuals fluctuates around some kind of equilibrium. In this paper we aim at predicting and understanding this equilibrium.

2.2 A naive estimate for the infected fraction

The SIS process on the complete graph K_n is a birth-death process and is quite well understood. For instance, the time to reach metastability is studied in [19], the average time until extinction in [40]. A slight modification of the process by forbidding the transition to the all-healthy state is considered in [8]. This gives a very accurate approximation of the metastable distribution of the SIS process, for which exact but somewhat implicit expressions are given. The metastable average infected fraction is $(1 - \lambda^{-1})n$ if the infection rate is $\tau = \lambda n^{-1}$ for some constant $\lambda > 1$, see [1, 42]. Convergence of the metastable infected fraction to a Gaussian with variance $\lambda^{-1}n$ is rigorously proved in [3]. This result can be used for a first naive estimate for the metastable infected fraction in an Erdős-Rényi graph.

Consider the SIS process with infection rate τ on the Erdős-Rényi graph $G_{n,p}$. An infected node can only infect a healthy node if there is an edge between them. Now assume that the event of two nodes being connected is independent of the event that exactly one of them is infected¹. The product $p\tau$ could then be

¹This assumption is reasonable if degrees are not too small. In reality we expect connected nodes to be positively correlated, i.e. if they are connected, it is less likely that exactly one of them is infected. We will come back to this issue later.

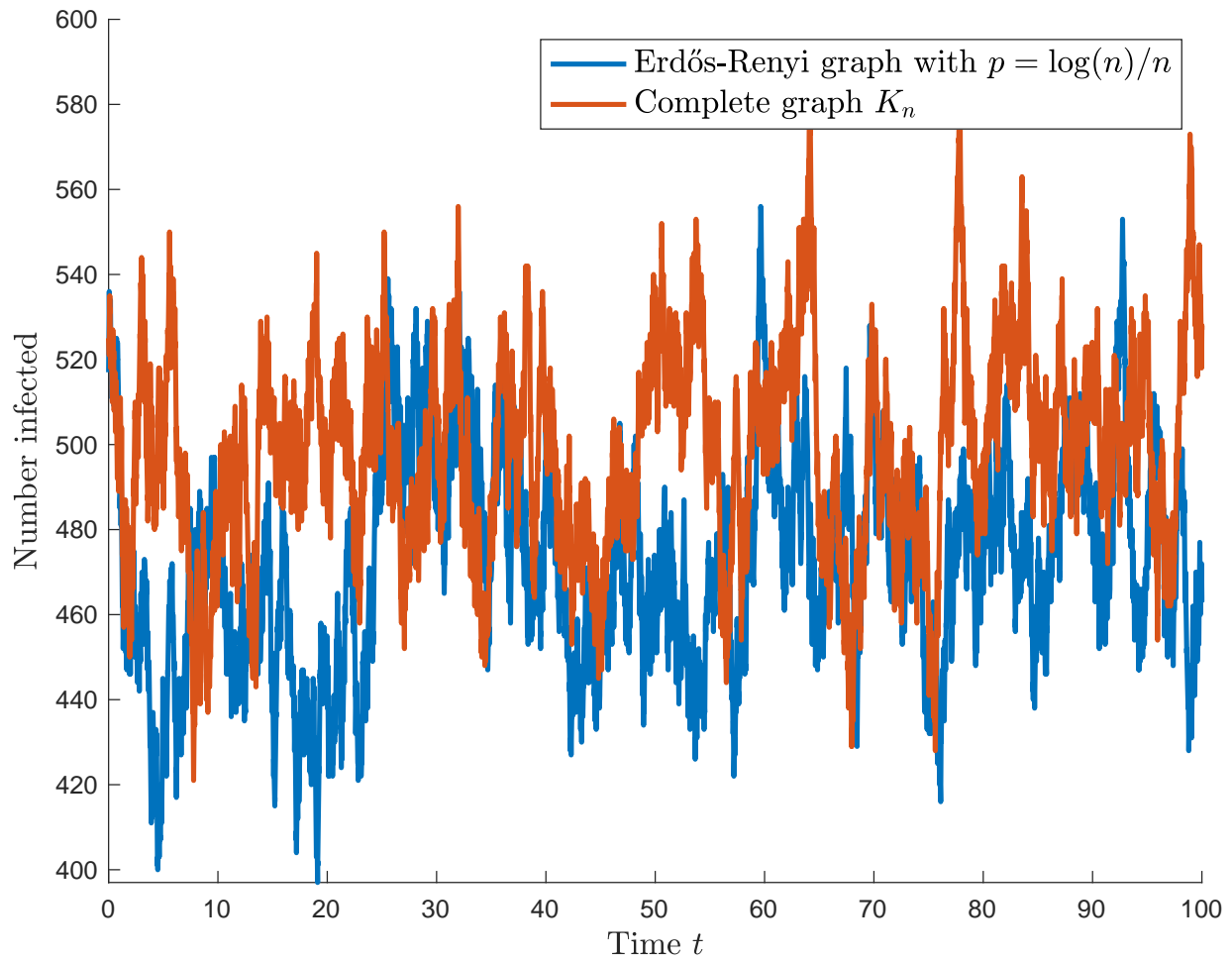


Figure 1: Number of infected nodes over time for the complete graph and an Erdős-Rényi graph. In both cases $n = 1000$ and the global infection rate $p\tau$ is equal to $2/n$, but the ER graph has a lower equilibrium.

interpreted as the expected infection rate between a random infected and a random healthy node and will be called the *global infection rate* of the process. Heuristically, the behaviour on an Erdős-Rényi graph with edge probability p and infection rate τ should be comparable to the behaviour on the complete graph with the same global infection rate. We therefore take $p\tau$ of order n^{-1} so that we can write $p\tau = \lambda n^{-1}$ for some constant $\lambda > 1$. Based on the heuristic that the global infection rate determines the quasi-stationary infected fraction, comparison with the complete graph (which is $G_{n,p}$ with $p = 1$) gives the following prediction

Heuristic 1. *Consider the SIS process on an Erdős-Rényi graph $G_{n,p}$ with global infection rate $p\tau = \lambda n^{-1}$. The quasi-stationary distribution satisfies*

$$X \sim N(\mu, \sigma^2), \quad \text{with } \mu = (1 - \lambda^{-1})n, \quad \sigma^2 = n\lambda^{-1}.$$

We could make this into a heuristic for the infected fraction, by dividing by n . This gives

$$\bar{X} \sim N(1 - \lambda^{-1}, (\lambda n)^{-1}),$$

so the infected fraction converges to $1 - \lambda^{-1}$ if $n \rightarrow \infty$. Heuristic 1 asymptotically gives the correct expectation if the degrees go to infinity ($np \rightarrow \infty$). This can be proved using birth-death chains and similar methods as in [6]. If np is constant, the expectation in Heuristic 1 is asymptotically incorrect. The variance is harder to control, we are not aware of any asymptotic results on the variance.

For efficiency of simulation, we will mostly restrict to the case $\lambda = 2$. We think that other choices give qualitatively similar behaviour. For an illustration of other values, see Figure 4 on page 8.

To assess Heuristic 1, Figure 1 compares a simulation of the process on an Erdős-Rényi graph with a simulation on K_n . At $t = 0$, each node is infected with probability $1/2$ independently. Taking the average over time, the process on the complete graph has half of the population infected (this has been rigorously proved in [3]). Heuristic 1 predicts the same for the Erdős-Rényi graph. Apparently, the average infected fraction in *this realization* of the Erdős-Rényi graph is lower, the picture shows an average around 470.

It could still be that the heuristic works well if we would average over multiple realizations of the Erdős-Rényi graph. We therefore repeated the simulation and generated 10 independent realizations of the Erdős-Rényi graph. On each of these graphs, we simulated the SIS process for $0 \leq t \leq 1000$. See Figure 2 for the (approximated) quasi-stationary distribution for each of the graphs and a comparison with the quasi-stationary distribution of the complete graph.

Based on Figure 2, there seems to be a systematic overestimation of the mean in Heuristic 1, which does not vanish if we would average over multiple realizations of the Erdős-Rényi graph. The mean of the quasi-stationary distribution is typically smaller than $n/2$. Apparently Heuristic 1 is too naive. One reason is that the infected set is not a uniform selection of nodes. This is an essential difference with the complete graph, where transition rates only depend on the size of the infected set, not on the exact selection of infected nodes. In Erdős-Rényi graphs, nodes with higher degrees are more likely to be in the infected set. Another point is that there are local effects: neighbors tend to be infected or healthy simultaneously. These differences make the model more realistic, but at the same time more complicated. We can not just take averages over all nodes as in the complete graph, but need more subtle estimation methods.

2.3 Annealed and quenched estimates

When looking at Figure 2, we see that the distribution in the Erdős-Rényi graph is not only clearly different from the complete graph, but also depends on the realization of the graph. For a given graph G , we can estimate the metastable distribution by simulating the SIS process on this particular graph. The corresponding random variable depends on G and on the infection rate τ and is denoted $X(G, \tau)$. Given G , the metastable mean infected number is a constant $\mu(G, \tau) := \mathbb{E}[X(G, \tau)]$. The expectation is taken with respect to the randomness of the process, not of the graph. We will call $\mu(G, \tau)$ the *quenched mean* and $\mu(G, \tau)/n$ the *quenched infected fraction*. Each blue curve in Figure 2 has its own quenched mean. Similarly, we denote the quenched variance by $\sigma^2(G, \tau)$.

If we take the graph to be random, then $\mu(G, \tau)$ becomes a random variable. Now we can take the expectation over the randomness of the graph as well to find the constant $\mathbb{E}[\mu(G, \tau)]$. This is what we will call the *annealed mean*. The annealed mean is independent of the graph realization and can be simulated by generating a bunch of graphs, running the process on each of them and taking the average of their

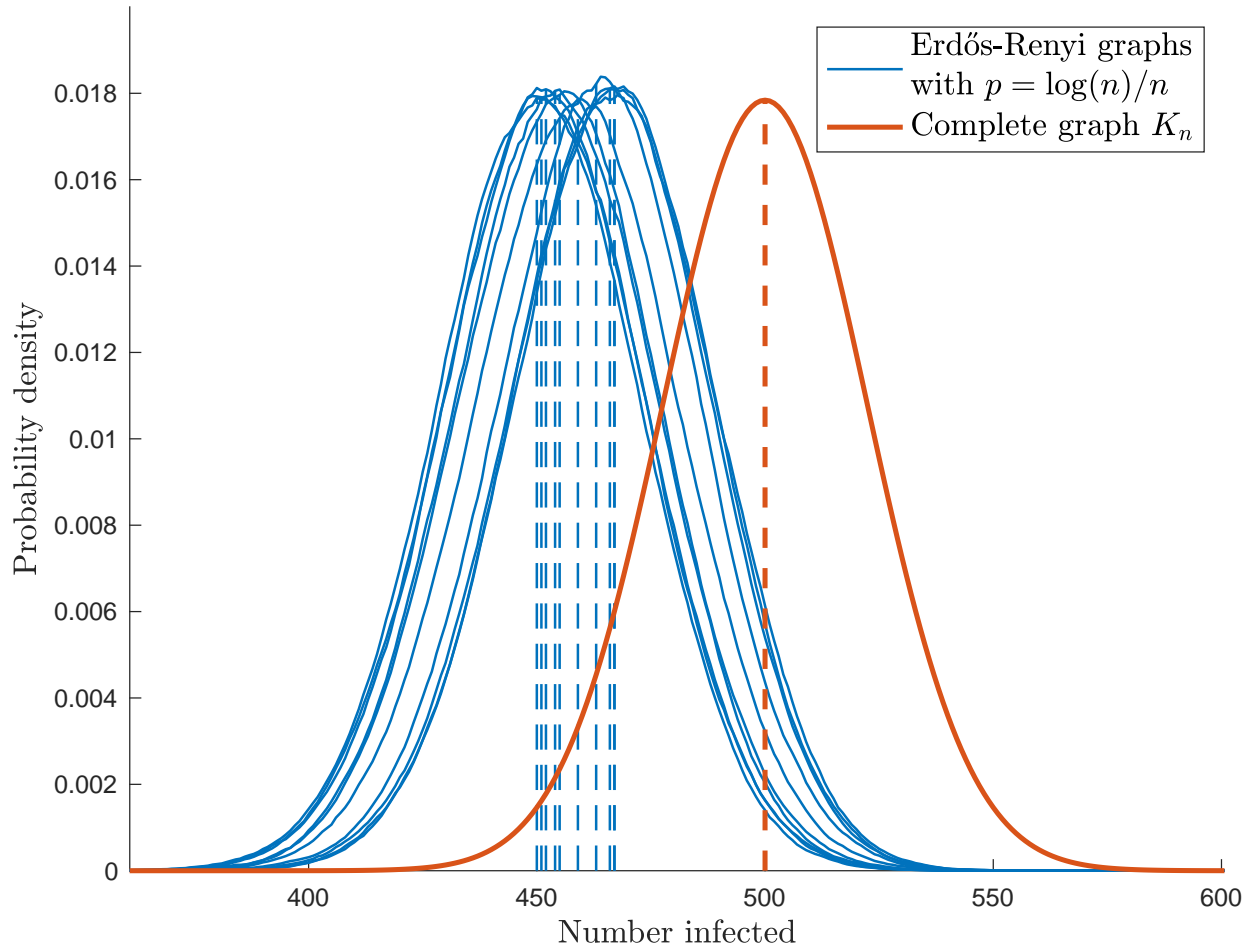


Figure 2: Probability distribution of the number of infected nodes in the complete graph (red) and in 10 realizations of the Erdős-Rényi graph (blue), all with $n = 1000$ and global infection rate $2/n$. Dashed lines indicate means.

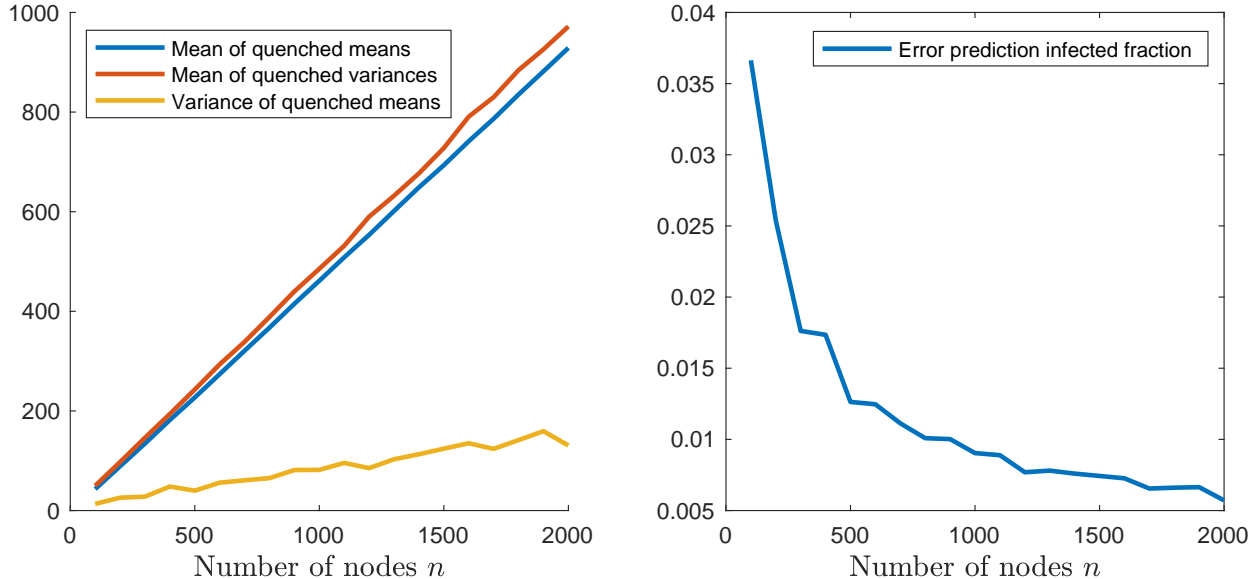


Figure 3: Left: Fixing an Erdős-Rényi graph ($p = \log(n)/n$, $p\tau = 2/n$), the metastable number of infected has mean (blue) and variance (red) both close to $n/2$. Varying the graph, the means themselves also fluctuate with a variance of order n (yellow). Right: Approximate minimal standard error for any annealed method to estimate a quenched infected fraction.

metastable quenched means. For the SIS process on Erdős-Rényi graphs, the annealed mean is a function of the parameters which we denote by $\mu(n, p, \tau)$.

This gives rise to two different questions concerning estimation of the metastable infected fraction (or other quantities) in $G = G_{n,p}$:

1. **Annealed estimation:** given n , p and τ , estimate $\mu(G, \tau)$, without observing the realization of G . The estimate will be a function $\hat{\mu}(n, p, \tau)$.
2. **Quenched estimation:** given the realization of G , estimate $\mu(G, \tau)$ using the graph information. The estimate will be a function $\hat{\mu}(G, \tau)$.

When doing quenched estimation, we are estimating the constant $\mu(G, \tau)$ for fixed G . The metastable infected fraction is some complicated function of G and τ which in principle could be determined exactly. However, when doing an annealed estimation, the realization of G is not known and $\mu(G, \tau)$ is a random variable. This implies that we will always make errors caused by the variation of this random variable. It therefore makes sense to investigate the order of the variance of $\mu(G, \tau)$ when G is random.

To do this, we generated for different values of n , realizations $G_n^{(1)}, \dots, G_n^{(100)}$ of an Erdős-Rényi graph $G_{n,p}$. On each of them, we simulated the quenched mean $\mu(G_n^{(k)}, \tau)$ and quenched variance $\sigma^2(G_n^{(k)}, \tau)$ of the metastable distribution. Then we took averages over k to obtain the mean of quenched means and the mean of quenched variances. Plotting them (Figure 3, left) shows that quenched means and quenched variances both grow linearly in n . In fact they are both close to $n/2$, as could be expected by comparing to the complete graph (cf. Heuristic 1).

Important is that also the variance of the quenched means appears to grow linearly with n . This indicates that annealed estimates for $\mu(G, \tau)$ will always have errors of the same order as fluctuations in the metastable distribution (i.e. the square root of the quenched variance). Therefore, graph information is for all graph sizes of significant importance to make accurate estimates. Taking the square root of the variance of the quenched means and dividing by n gives the standard deviation in annealed estimation of $\mu(G, \tau)$, see right plot in Figure 3. For instance, for $n = 1000$, the standard deviation is about 0.01. This implies that any annealed estimation method for the infected fraction will make errors of at least this order.

This point is once again illustrated in Figure 4. Here we see simulations of infected fractions in Erdős-Rényi graphs for different values of p and λ . Some of these estimates are annealed (corresponding to the

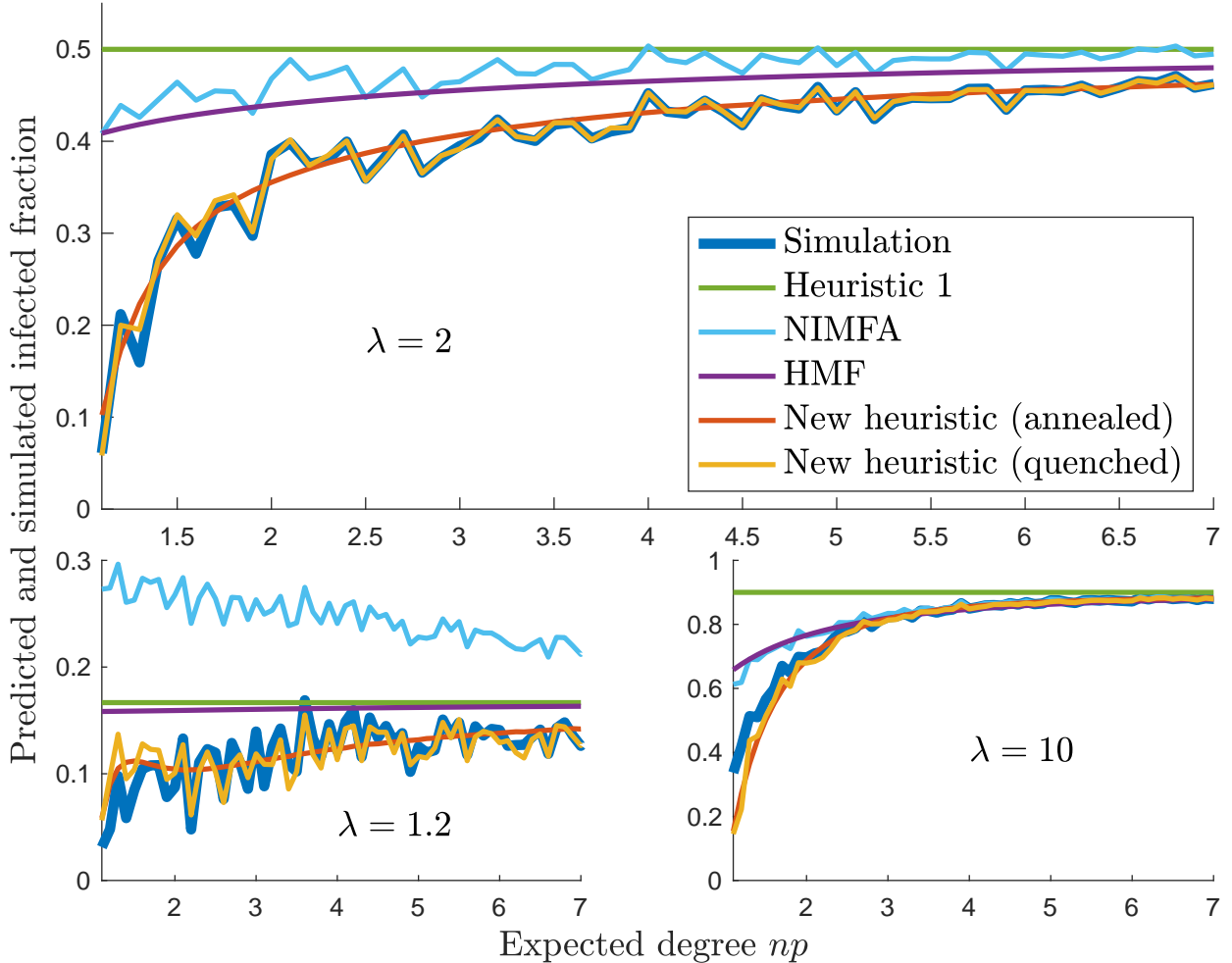


Figure 4: Simulated infected fraction compared to different estimates. In all cases, $n = 1000$. Annealed methods are smooth, quenched methods follow the fluctuations of the simulation.

smooth curves) and some of them are quenched (the non-smooth curves). The quenched estimates fluctuate much more, but follow the simulation result much better. An annealed estimate can never reproduce these fluctuations, because they are caused by the randomness of the graph.

Figure 4 also shows that HMF systematically overestimates the infected fraction in these sparse graphs. The same holds for NIMFA, although it clearly follows the random fluctuations of the simulation due to the quenched nature of NIMFA. The new heuristics presented in this paper are much more accurate, both their annealed and quenched versions.

2.4 Main results

The main result of this paper is a new method to estimate the infected fraction for connected graphs:

Main result. *Algorithm (details in Figure 17 on page 26) to estimate the metastable infected fraction μ/n in a connected graph G . **Input:** Degree sequence of G , infection rate. **Output:** Prediction for μ/n .*

This algorithm and variants of it will be mathematically motivated and discussed in detail in Section 4. The algorithm in Figure 17 is quenched, since it uses the degree sequence. An important variant is the annealed algorithm: for parametric random graph models, one first estimates the degree frequencies, and then the algorithm is applied to the estimated degree sequence.

For graphs which are not connected, but have a unique giant component, the algorithm can be applied to this giant component. This is the case for sparse Erdős-Rényi graphs, see Section 5.1.

The algorithm also gives the tools to estimate quantities other than the infected fraction, like fluctuations around the metastable equilibrium and correlations between neighboring nodes, see Section 5.2.

Power and limitations The algorithm is designed for graphs which are locally tree-like and have a degree distribution with exponential tails. This includes Erdős-Rényi graphs, random regular graphs and configuration model graphs with suitable degrees. Ultimately, the algorithm relies on the mean field assumption that pairs of nodes with the same pair of degrees have a similar neighborhood which can be well approximated by an ‘average neighborhood’. This assumption might fail if there are some nodes with very high degree, like in power-law random graphs. Also for grids the algorithm is not expected to work very well, since the grid structure induces much stronger local correlations than a tree.

The main power of our algorithm is that it incorporates correlations, while still being computationally feasible. In dense graphs, HMF and NIMFA perform quite well. However, it gets more and more delicate to make accurate estimates when graphs get sparser. Sparseness makes averages less reliable, correlations more important and heuristics more sensitive to errors. Our algorithm extends HMF by incorporating correlations. We did extensive simulations (Section 5), which show that in sparse Erdős-Rényi graphs the algorithm is much more accurate than HMF and NIMFA (cf. Figure 4). Higher order methods improve the accuracy, but complicate the model. In practice, a higher order method therefore is often used in an approximate form. The challenge is to reduce the complexity, while still capturing the essential information. We address this problem by a degree-based second order method. Since it is based on pairs of degrees rather than pairs of nodes, the number of variables in the system stays limited.

The quenched variants of our algorithm typically give more accurate results than the annealed versions, at the cost of more complicated computations. The most advanced quenched version would use the full graph structure and would be an extension of NIMFA. It seems however that the same quality of estimation can already be reached by simpler variants, using only the degree sequence or even only the sum of the degrees (for Erdős-Rényi graphs this works well).

Computation time Our method introduces for each pair of degrees of neighbors a small system of linear equations. These systems can be solved independently. These equations also depend on a few global parameters, which can be found by an iterative procedure.

Figure 5 compares the computation time for different algorithms (the same as in Figure 4, exact definitions follow later). All computations were done on a normal work laptop. The cheapest algorithms are the annealed algorithms. They require to first compute the binomial probabilities. For degrees greater than twice the expectation, the probability is negligible in this case and approximated by 0. The remaining probabilities are numerically approximated. For HMF, one then has to solve a single non-linear equation. Up to size $n = 2^{28}$, the whole computation requires only a fraction of a second.

The annealed version of our new heuristic is slightly more complicated. Instead of solving one non-linear equation, we have to simultaneously solve about $(2 \log(n))^2$ linear systems of four equations with four unknowns and two non-linear equations. Still, the solution is found in less 0.1 seconds for graph sizes up to $n = 2^{28}$. The bottleneck for these two annealed methods is the maximal size of numbers the system is able to handle. The computation time itself only grows very slowly with n .

The next method in order of computational complexity is the quenched version of our new heuristic. For this method, we generate a graph and use the actual degree sequence. The most demanding part of the computation is counting to find the degree frequencies (linear in n). For graph sizes up to $n = 2^{16}$, the algorithm is still completed in less than a second. Bigger graph sizes were out of reach, because memory capacity did not allow for it. For these sparse graphs, the memory size needed grows like $n \cdot \log(n)$. For denser graphs memory space of order n^2 might be needed.

The problem of memory also appears when doing simulations. A simulation of 10^3 time units of the SIS process on $n = 2^{16}$ nodes is completed in a few minutes. Memory restrictions are more of an issue than computation time. It has to be noted here that our choice of infection rate allows for a particularly efficient implementation. Other choices for p and τ might make it harder to run the simulation, both in terms of memory and computation time.

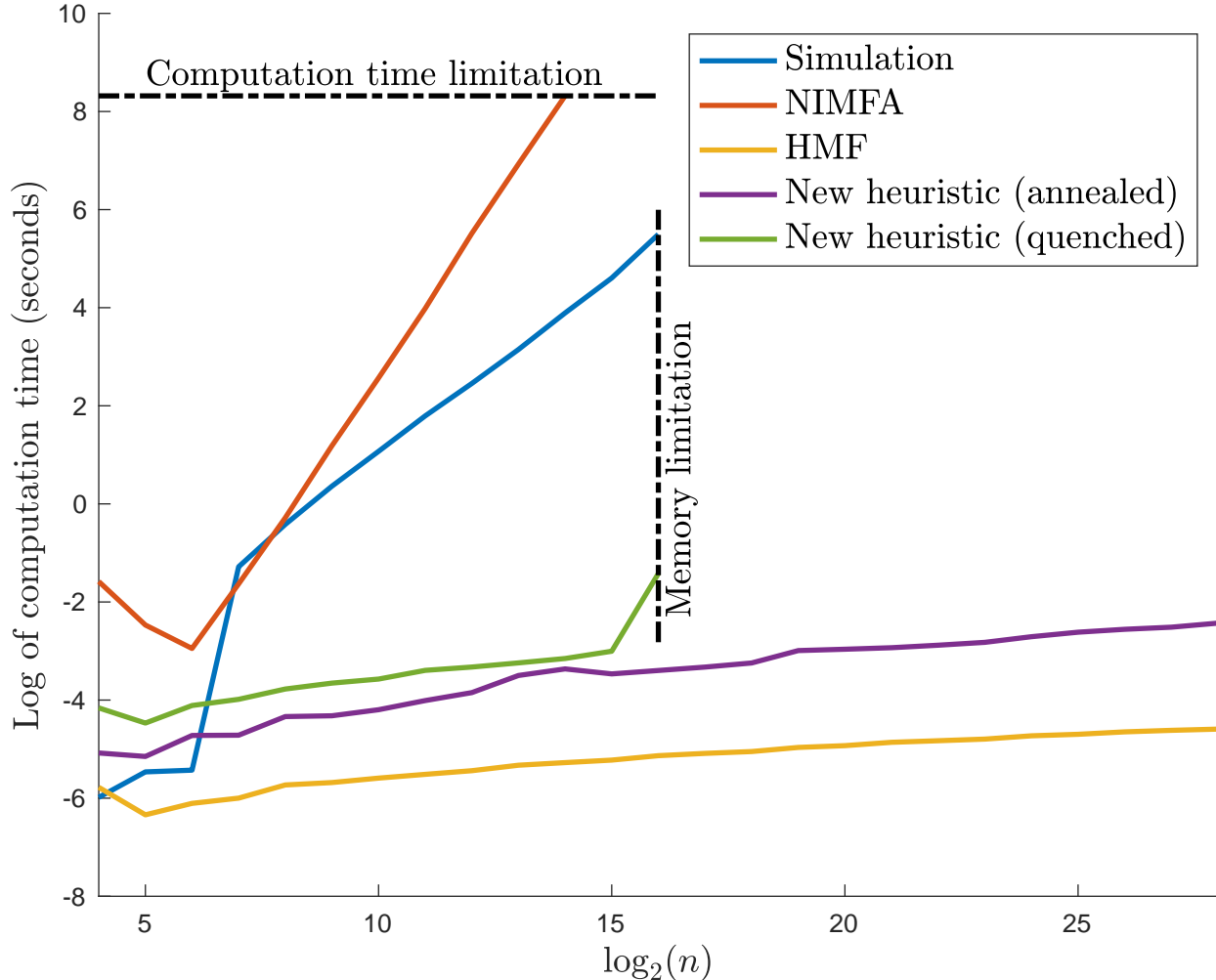


Figure 5: Comparison of computation times for Erdős-Rényi graphs with $p = \log(n)/n$ and $\lambda = 2$. NIMFA needs a lot of time. Quenched methods and simulation need a lot of memory.

Finally, NIMFA requires to solve a non-linear system of n equations in n unknowns. Now computation time really becomes the deciding factor. Doing the computation for $n = 2^{14}$ already takes more than one hour. The methods in [7, 17] which do try to incorporate correlations are even much worse from a computational point of view.

3 Improved heuristics for the infected fraction

In this section we start to gradually build towards our main estimation method which will be presented in Section 4. We show how to use the degrees to design more accurate estimation methods. One of these methods will turn out to be equivalent to NIMFA, another to HMF.

The methods in this section, although much better than Heuristic 1, still have their shortcomings. We will explain where it goes wrong, and in particular why NIMFA and HMF have a serious bias in sparse graphs. Nevertheless, the ideas in this section are the basis for the exposition of more sophisticated methods in Section 4.

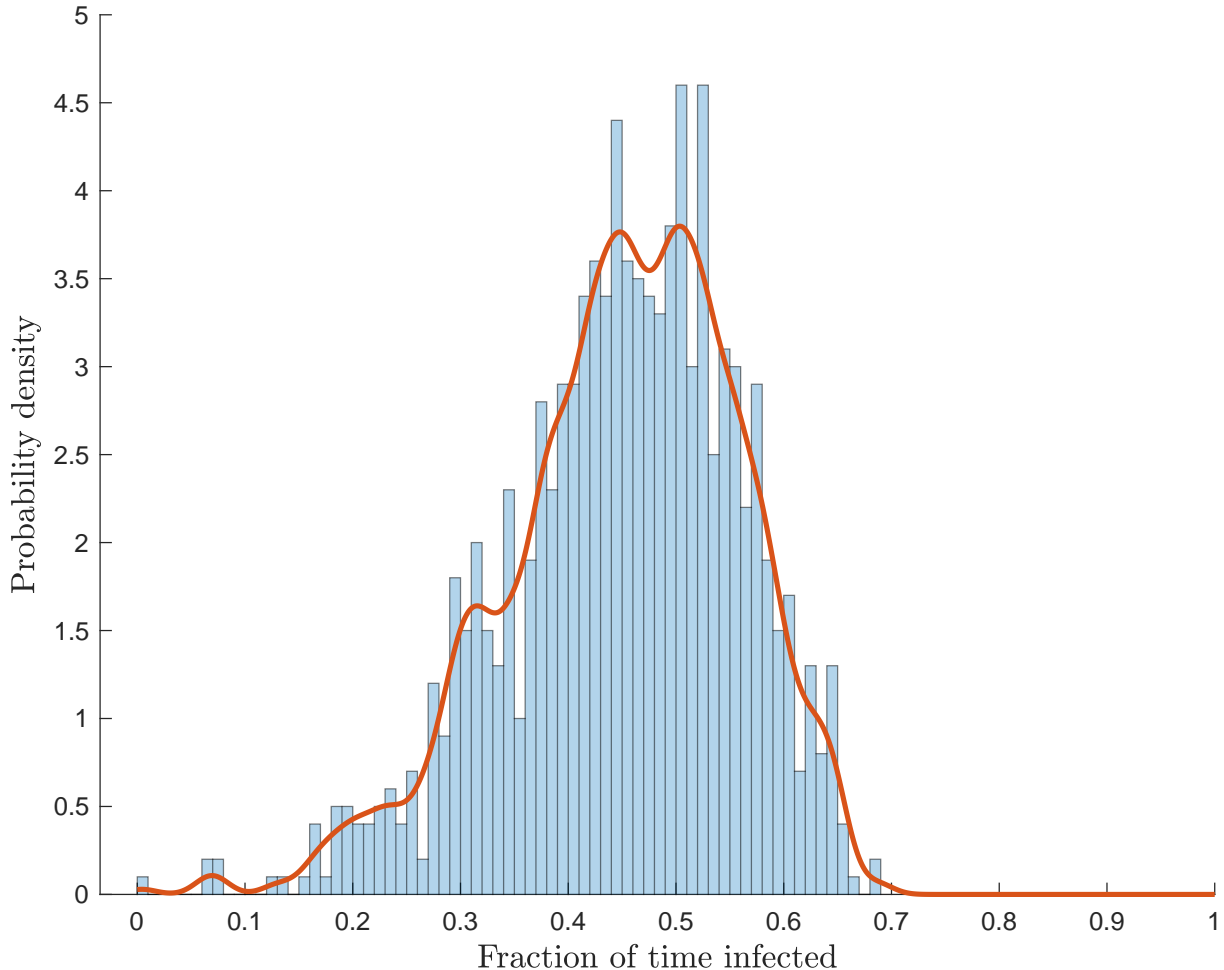


Figure 6: Simulated and estimated probability density of the fraction of time a node is infected (ER graph with $n = 1000$, $p = \log(n)/n$, $\lambda = 2$).

3.1 Nodes with higher degree are more frequently infected

Both in the Erdős-Rényi graph and in the complete graph, the fraction of nodes that is infected is quite stable over time, see again Figure 1. Since nodes are indistinguishable in the complete graph, each individual node is expected to be infected the same fraction of time. In the complete graph ($n = 1000$, $\lambda = 2$), *all* nodes are infected about half of the time. If we send the running time (not too fast, to avoid extinction) and the number of nodes to infinity, this fraction of time will converge to $1/2$ for each individual node. To illustrate, we ran the process on the complete graph for 10^5 units of time and found that 99% of the nodes was infected between 49.5 and 50.3% of the time.

The fraction of time an individual node is infected could be quite different in the Erdős-Rényi graph. In Figure 6, we see a histogram of these fractions of time and an estimate of the density function (using kernel density estimation). In this Erdős-Rényi graph, nodes are only *on average* infected about half of the time. The fraction of time an individual node is infected ranges from 0 to about 0.7. For each individual node it will converge if the running time of the process increases, but the limiting fraction for each node will depend on the geometry of the graph.

The degree of a node can be used to give quite a good estimate for the fraction of time this node will be infected. This in turn will explain the shape of the density function in Figure 6. In first approximation, the fraction of time a randomly picked node is infected is equal to $1 - \lambda^{-1}$. It therefore infects each of its neighbors at rate $\tau - \tau\lambda^{-1}$.

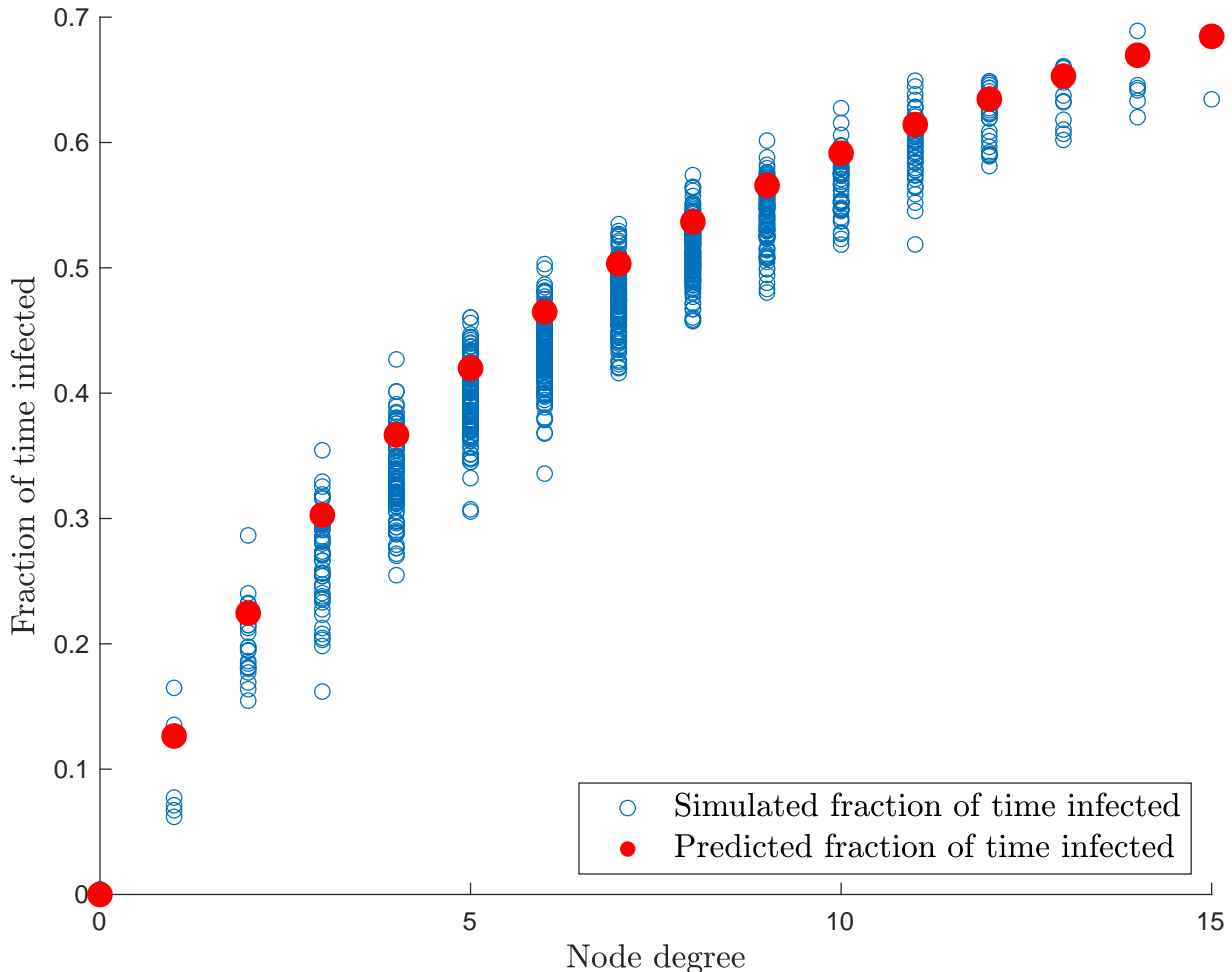


Figure 7: Simulation of the fraction of time nodes are infected, plotted as points (d_i, f_i) in blue (ER graph with $n = 1000$, $p = \log(n)/n$, $\lambda = 2$). The red markers indicate the degree-dependent estimate $(d, f(d))$ based on the heuristic (1).

Let i be a random node with degree $d = d_i$. The fraction of time this node is infected will be called f_i . Assume that its neighbors are ‘random’ nodes. Then i is healing at rate 1 and, since it has d neighbors, getting infected at rate $d\tau - d\tau\lambda^{-1}$.

If we consider a Markov process with one node, which is healing at rate 1 and getting infected at rate α , in the stationary distribution this node is infected a fraction $\alpha/(1 + \alpha)$ of time. Therefore, in our more complicated model, the fraction of time i is infected is estimated by

$$\hat{f}_i := \frac{d\tau - \frac{d\tau}{\lambda}}{1 + d\tau - \frac{d\tau}{\lambda}}. \quad (1)$$

Fixing the parameters of the graph and the process, this estimate only depends on d , so we write $f(d)$ for \hat{f}_i . In Figure 7, we plotted the points $(d, f(d))$ and compare with all the points (d_i, f_i) obtained by simulation.

In Figure 8, we compare the empirical distribution function of the per-node infected fraction of time, $\frac{1}{n} \sum_{i=1}^n \mathbb{1}\{f_i \leq x\}$, with the quenched estimated cumulative distribution function $\frac{1}{n} \sum_{i=1}^n \mathbb{1}\{f(d(i)) \leq x\}$.

To compute this estimation, we need the actual degrees in the graph. Since we know that the degree distribution D in the graph is $\text{Bin}(n - 1, p)$, we can also estimate the distribution without observing the

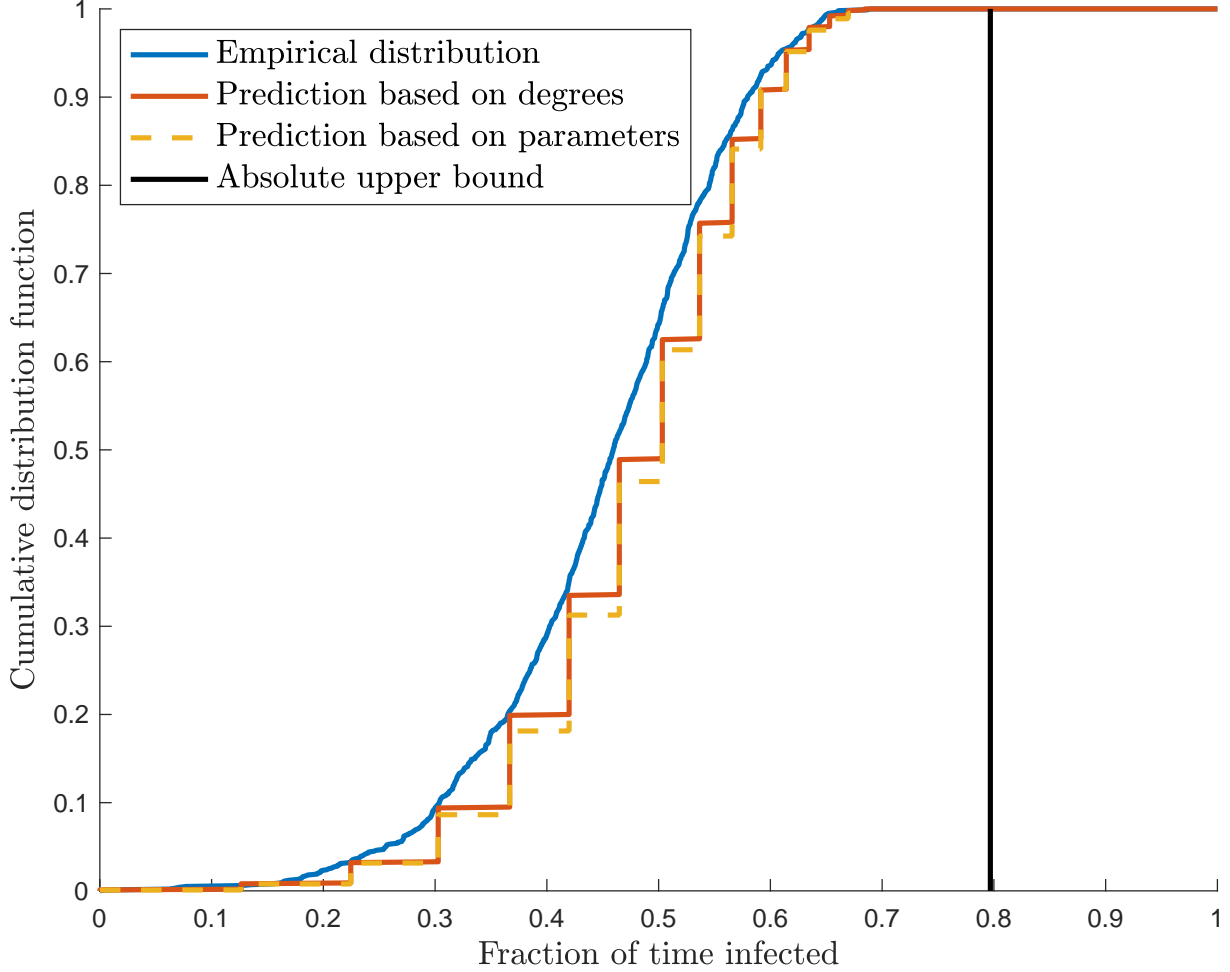


Figure 8: Cumulative distribution of infected fraction of time (ER graph with $n = 1000$, $p = \log(n)/n$, $\lambda = 2$). Blue: empirical. Red: quenched estimate. Yellow: annealed estimate. Both estimates have jumps at the values $f(d)$. Black: absolute upper bound for the infected fraction caused by the maximal degree.

actual degrees by

$$\begin{aligned}
 \frac{1}{n} \sum_{i=1}^n \mathbb{1}\{f(d(i)) \leq x\} &= \sum_{d=0}^{n-1} \frac{\#\{i : d_i = d\}}{n} \cdot \mathbb{1}\{f(d) \leq x\} \\
 &\approx \sum_{d=0}^{n-1} \binom{n-1}{d} p^d (1-p)^{n-1-d} \cdot \mathbb{1}\{f(d) \leq x\}.
 \end{aligned} \tag{2}$$

This estimate as well is compared with the observed empirical distribution in Figure 8. Note that this is an annealed estimate: it can be computed using only the three parameters n , p and τ .

If the maximal degree Δ in the graph is known, we can compute an absolute upper bound for the (limiting) fraction of time a node is infected. Let θ be the maximal fraction of time a node is infected. Let i be a node in the graph. If all its neighbors are infected all the time, then i is infected at rate at most $\Delta\tau$. It follows that $\theta \leq \Delta\tau/(1 + \Delta\tau) < 1$.

A sharper heuristic upper bound is obtained by the using positive correlations between i and its neighbors (shown in [11, 9]). The neighbors of i also are infected at most a fraction θ of time. Positive correlations mean that this upper bound still holds when restricting to periods when i is healthy. Therefore, i is infected

at rate at most $\Delta\tau\theta$. This implies that $\theta \leq \Delta\tau\theta/(1 + \Delta\tau\theta)$. It follows that θ is at most equal to the largest solution of this equation, which is given by $(\tau\Delta - 1)/(\tau\Delta)$.

In our example in Figure 8, we have $\tau = 2/(np) = 2/\log(1000) \approx 0.29$ and $\Delta = 17$. This gives approximately 0.79 as an absolute upper bound for the fraction of time a node can be infected, see the vertical line in the plot.

Note that $\Delta = n - 1$ in the complete graph K_n , giving the upper bound $1 - 1/((n - 1)\tau) \approx 1 - 1/\lambda$. This is consistent with known results for K_n .

3.2 Degree-based heuristics for the infected fraction

The idea of estimate (1) will be used to estimate the infected fraction $\mu/n = \mathbb{E}\bar{X}$ of the population. Let i be a node with degree d and assume that its neighbors are infected a fraction μ/n of time. Analogous to (1), we estimate the fraction of time i is infected by

$$\hat{f}_i := \frac{d\tau\mu/n}{1 + d\tau\mu/n}. \quad (3)$$

A very similar formula is derived in [35], as the stationary solution of the differential equation

$$\partial_t f(d, t) = -f(d, t) + \tau d(1 - f(d, t))\Theta(t). \quad (4)$$

Here $f(d, t)$ is the probability a node of degree d is infected at time t , and $\Theta(t)$ is the fraction of half-edges connected to an infected node. Note that $\Theta(t)$ is not exactly the same as the infected fraction of the population at time t . We will come back to this in Section 3.3. In stationarity, $\Theta(t)$ does not depend on t , and setting the derivative in (4) equal to zero gives the analogue of (3).

Averaging the quantity \hat{f}_i over all nodes in the graph, we obtain an estimate for μ/n . Hence, if n , p and τ are given, μ/n can be estimated by (numerically) solving

$$\frac{\mu}{n} \approx \sum_{d=0}^{n-1} \binom{n-1}{d} p^d (1-p)^{n-1-d} \cdot \frac{d\tau\mu}{n + d\tau\mu}. \quad (5)$$

In fact the right hand side is the expectation $\mathbb{E}[\tau\mu D/(n + \tau\mu D)]$. Therefore, by Jensen's inequality, (5) implies $\mu/n \leq \tau\mu\mathbb{E}[D]/(n + \tau\mu\mathbb{E}[D])$. Solving for μ/n gives $\mu/n \leq 1 - \lambda^{-1}$, so that this procedure to estimate the infected fraction always gives a lower estimate than Heuristic 1.

For large n and d , the binomial probabilities in (5) are hard to compute, but they are well approximated by using the central limit theorem. This gives us

Heuristic 2. Consider the SIS process on an Erdős-Rényi graph $G = G_{n,p}$ with infection rate τ . The quasi-stationary infected fraction μ/n satisfies

$$\frac{\mu}{n} = \sum_{d=0}^{n-1} P(n, p, d) \cdot \frac{d\tau\mu}{n + d\tau\mu}. \quad (6)$$

Here $P(n, p, d)$ is either

(a) The probability $\mathbb{P}(\text{Bin}(n-1, p) = d)$ or an approximation to it (as in (5)).

(b) The exact frequency $\#\{i : d_i = d\}/n$.

Note that (a) gives an annealed estimate, while (b) is a quenched estimate. In view of earlier discussions, we expect (b) to be more accurate.

For $n \rightarrow \infty$, the probability mass of the degree distribution concentrates around its expectation np with standard deviation $\sqrt{np(1-p)}$. This means that for $np \rightarrow \infty$ and $\tau np = \lambda$ the right hand side of (6) converges to

$$\lim_{n \rightarrow \infty} \frac{np\tau\mu}{n + np\tau\mu} = \frac{\lambda \lim_{n \rightarrow \infty} \mu/n}{1 + \lambda \lim_{n \rightarrow \infty} \mu/n}.$$

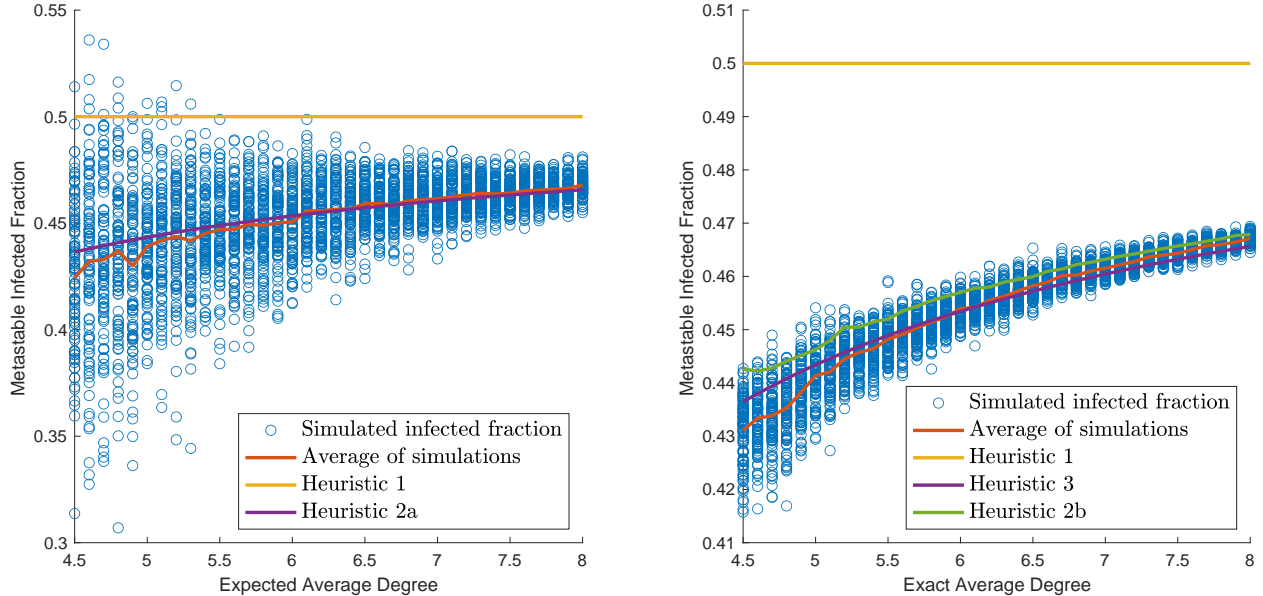


Figure 9: Infected fractions in Erdős-Rényi graphs with $p = \log(n)/n$ and $\lambda = 2$. Left: annealed estimate. Right: quenched estimate (the horizontal coordinate of each point depends on the graph.)

Solving (6) for $\lim_{n \rightarrow \infty} \mu/n$, we obtain

$$\lim_{n \rightarrow \infty} \frac{\mu}{n} = 1 - \frac{1}{\lambda}, \quad (7)$$

so that both versions of Heuristic 2 coincide with Heuristic 1 for $n \rightarrow \infty$.

3.2.1 Simulation and annealed estimation for $p = \log(n)/n$

We test Heuristic 2a, taking edge probability $p = \log(n)/n$ and using the normal approximation. For each $n = \lceil e^{k/10} \rceil$, $k = 45, 46, \dots, 80$, we generate 100 replications of the Erdős-Rényi graph so that in total we have 3600 graphs. The average degrees vary from 4.5 to 8 and the sizes range from 91 to 2981 nodes. On each of those graphs, we simulate the SIS process with infection rate $\tau = 2/\log(n)$.

Our simulation results are given in Figure 9, left plot. Each simulated graph is represented by a small blue circle. The horizontal coordinate is the expected average degree $\log(n)$. The vertical coordinate is the simulated infected fraction \bar{X} , averaged over time. This is an estimate for the quasi-stationary mean. The variance is decreasing, since the graph sizes are increasing from left to right.

3.2.2 Using graph information: quenched estimates

Heuristic 2a seems to do quite well on average in Figure 9, but there is a lot of variation in the simulation results. The estimate by Heuristic 2a can be made *before* generating the graph. Can we estimate the stationary infected fraction more accurately *after* generating the graph and using characteristics of the graph?

To test this, we again generated Erdős-Rényi graphs with the same numbers of nodes as in Figure 9. If $p = \log(n)/n$, the expected total number of edges is $p \binom{n}{2} = \frac{1}{2}(n-1)\log(n)$. This time we conditioned the graphs to have the number of edges exactly equal to its (rounded) expectation. We can even eliminate the rounding error by slightly adjusting p . The simulation results are shown in Figure 9, right plot. The horizontal coordinate now is the *exact* average degree, since we fixed the number of edges to its expectation. For unconditioned ER graphs, this exact average degree is a quenched parameter, which can only be computed after observing the graph.

It turns out that graphs with the same exact average degree have a lot less variation in their quasi-stationary means than graphs merely having the same expected average degree. A lot of the variation is

explained by variation of the number of edges in the graph. The estimate therefore becomes more accurate by the following quenched estimation method: first estimate p based on the observed number of edges, then use this adjusted p for estimating the metastable infected fraction. The resulting heuristic is:

Heuristic 3. *Let G be an Erdős-Rényi graph with n nodes and m edges. Consider the SIS process on G with infection rate τ . The quasi-stationary infected fraction μ/n satisfies*

$$\frac{\mu}{n} = \sum_{d=0}^{n-1} P\left(n, \frac{m}{\binom{n}{2}}, d\right) \cdot \frac{d\tau\mu}{n + d\tau\mu}. \quad (8)$$

Here $P(n, p, d)$ is (an approximation to) the probability $\mathbb{P}(\text{Bin}(n-1, p) = d)$.

For the figures, we use the normal approximation. This estimate still seems to have a small systematic bias for some values of n . We will discuss systematic errors in Heuristic 2 and 3 in the next section.

Heuristic 3 uses the exact number of edges in the graph, which is equivalent to using the sum of the degrees. Next steps would be to use all individual degrees or even the full adjacency matrix A of the graph. If the full degree sequence is known, we could use Heuristic 2b with the exact numbers $\#\{i : d_i = d\}$. It turns out by simulations that this is more accurate than Heuristic 2a, but has a larger bias than Heuristic 3 in the simulated range, see again Figure 9. A remark to be made here is that now graphs with the same exact average degree might get different estimates. The curve for Heuristic 2b only shows the average of these estimates. This means that estimation errors for individual graph realizations can not be seen in the picture.

To see individual errors, we simulated the SIS process on 100 Erdős-Rényi graphs with $n = 1000$ nodes, $p = \log(n)/n$ and $\lambda = 2$. Figure 10 gives boxplots for the errors: the difference between the estimated infected fraction and the simulated infected fraction for the different heuristics. The errors for the annealed heuristics have much more variation. On the other hand, more detailed information than the number of edges does not really improve the estimation: Heuristic 3 is not worse than Heuristic 2b and 4 (these heuristics respectively use the exact number of edges, the exact degrees and the full adjacency matrix). Heuristic 4 (to be discussed next) has a small variation, but a large systematic error. The systematic errors of Heuristics 3 and 2b are relatively small, but the situation gets worse when the graph is more sparse, in particular when the graph disconnects. In that case one has to be more careful, see Section 5. In general, these heuristics work quite well on graphs which are fairly homogeneous such as the complete graph or Erdős-Rényi graph with enough edges. For less homogeneous graphs like power-law graphs, other heuristics are needed.

Now assume the full adjacency matrix is known. Writing again f_i for the fraction of time i is infected, and assuming independence between nodes, we find that i gets infected at rate $\tau \sum_{j:i \sim j} f_j$. Therefore f_i satisfies

$$f_i = \frac{\tau \sum_{j:i \sim j} f_j}{1 + \tau \sum_{j:i \sim j} f_j}. \quad (9)$$

It turns out that this is equivalent to NIMFA, which is derived as follows. Consider $\mathbb{P}(X_i(t) = 1) = \mathbb{E}[X_i(t)]$. By standard Markov chain theory, its derivative is expressed in the transition rates by

$$\frac{d}{dt} \mathbb{E}[X_i(t)] = -\mathbb{E}[X_i(t)] + \tau \sum_{j:i \sim j} \mathbb{E}[(1 - X_i(t)) \cdot X_j(t)],$$

where the first term on the right corresponds to healing of i and the second to infection. The NIMFA assumption is to ignore correlations by setting

$$\mathbb{E}[X_i(t) \cdot X_j(t)] = \mathbb{E}[X_i(t)] \cdot \mathbb{E}[X_j(t)]. \quad (10)$$

The stationary solution is then obtained by solving

$$0 = -\mathbb{E}[X_i] + \tau \sum_{j:i \sim j} \mathbb{E}[X_j] + \tau \mathbb{E}[X_i] \sum_{j:i \sim j} \mathbb{E}[X_j], \quad (11)$$

which is the same as (9). Solving this system of n non-linear equations and n unknowns gives a quenched estimate \hat{f}_i , after which the infected fraction of the population can be estimated by

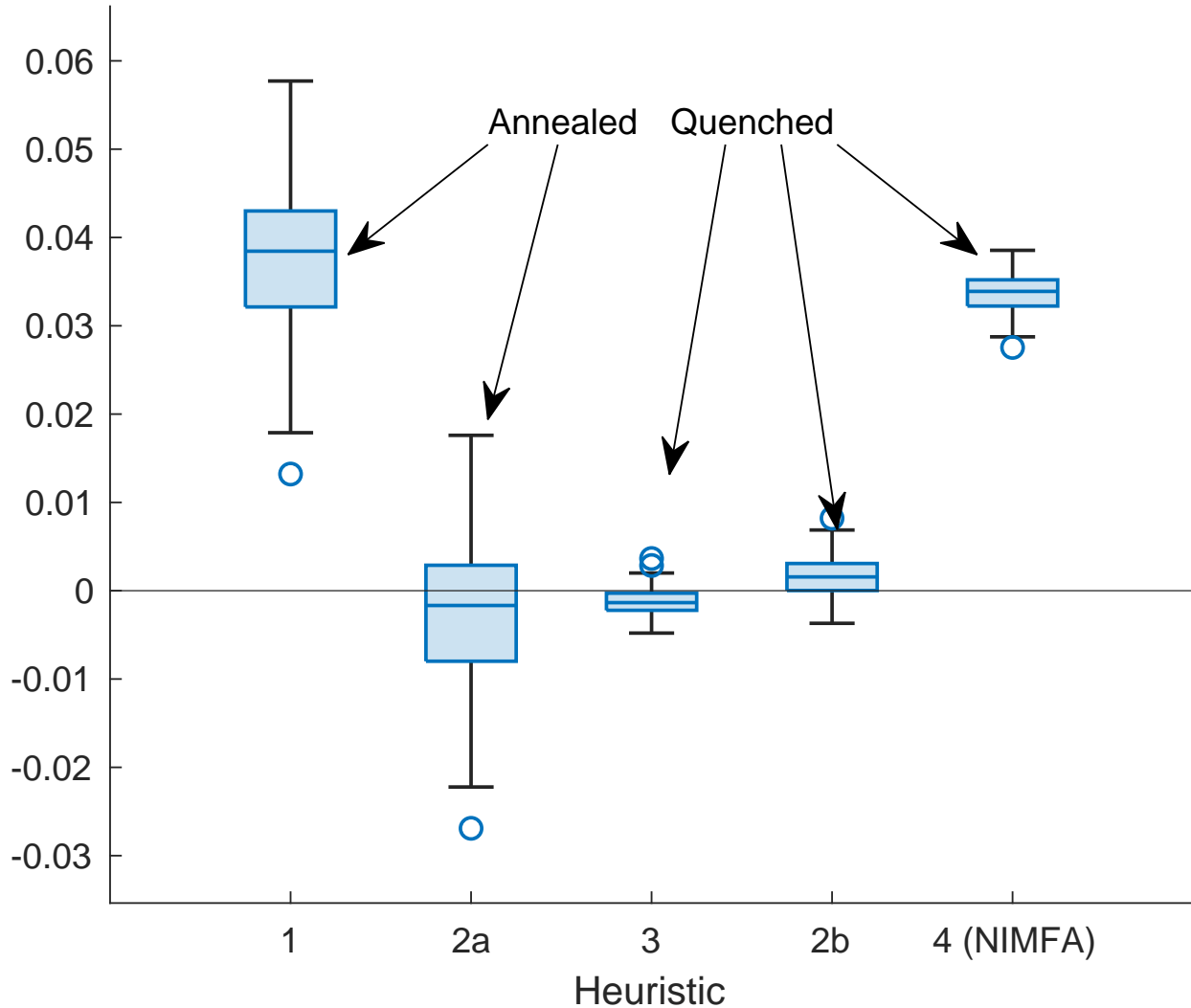


Figure 10: Error boxplots for each heuristic for Erdős-Rényi graphs with $n = 1000$, $p = \log(n)/n$ and $\lambda = 2$. The errors of annealed methods have a standard deviation of about 0.01, cf. Figure 3. The errors of quenched heuristics have smaller variation. Heuristic 1 and NIMFA are clearly biased.

Heuristic 4 (NIMFA). Let $G = (V, E)$ be an Erdős-Rényi graph. Consider the SIS process on G with infection rate τ . Let $\hat{f}_i, i \in V$ be the solution of the system (9). The quasi-stationary infected fraction μ/n satisfies

$$\frac{\mu}{n} = \frac{1}{n} \sum_{i=1}^n \hat{f}_i. \quad (12)$$

One would expect this to be more accurate than Heuristic 2b. However, our simulations show NIMFA to be strikingly more biased for $n = 1000$ and $p = \log(n)/n$ (see Figure 10). This is a general problem with NIMFA in graphs with small degrees. In the next sections we explain how this is possible.

3.3 Systematic errors I: size bias and the infection paradox

Heuristics 2a, 2b and 3 are all based on the assumption that the neighbors of a random node i are infected a fraction μ/n of time. However, given the information that j is a neighbor of i , the degree distribution of j is different. This is the so-called friendship paradox, and the degree distribution of j is called the excess

degree distribution or size biased distribution [31, 41]). Precisely, the probability that j has degree d has to be weighted by a factor d . When all nodes independently have the same degree distribution D , the degree D_j of j satisfies

$$\mathbb{P}(D_j = d \mid i \sim j) = \frac{d \cdot \mathbb{P}(D = d)}{\mathbb{E}[D]}. \quad (13)$$

For the Erdős-Rényi graph, an exact expression is

$$\mathbb{P}(D_j = d \mid i \sim j) = \binom{n-2}{d-1} p^{d-1} (1-p)^{n-d-1}. \quad (14)$$

For large n and small p and d , this results in

$$\mathbb{P}(D_j = d \mid i \sim j) \approx \frac{(np)^{d-1} (1-p)^n}{(d-1)!} \approx \frac{d \cdot \mathbb{P}(D_i = d)}{np}, \quad (15)$$

which is consistent with the general formula (13). Note that the formula in the middle is also approximately $\mathbb{P}(D_i = d-1)$, so that the degree distribution of j is obtained by shifting the original degree distribution by 1. Hence, in Heuristics 2a, 2b and 3 we make an error of 1 in counting the neighbors of j . This error causes an underestimation of the fraction of time neighbors of i are infected, which in turn also leads to underestimation for i itself.

The friendship paradox thus implies an infection paradox (illustrated in Figure 11):

Paradox 1. *An average neighbor of an average node is more often infected than the node itself.*

Instead of assuming that i and j themselves have the same degree distribution, it is better assume that neighbors of j have the same degree distribution as neighbors of i . Note that this assumption is still not entirely correct, we now essentially make an error of 1 in counting neighbors at distance 2 of j . In a locally tree-like graph this error is of a smaller order. Under this improved assumption, we obtain

$$\frac{\tilde{\mu}}{n} = \sum_{d=1}^{n-1} \mathbb{P}(\text{Bin}(n-2, p) = d-1) \cdot \frac{d\tau\tilde{\mu}}{n + d\tau\tilde{\mu}} \quad (16)$$

where $\tilde{\mu}/n$ is the fraction of time a random neighbor of a random node is infected. This motivates to adapt Heuristic 2 and to estimate μ/n by

Heuristic 2 (Variant HMF). *Solve (16) for $\tilde{\mu}$. Then μ satisfies*

$$\frac{\mu}{n} = \sum_{d=0}^{n-1} \mathbb{P}(\text{Bin}(n-1, p) = d) \cdot \frac{d\tau\tilde{\mu}}{n + d\tau\tilde{\mu}}. \quad (17)$$

In fact, $\tilde{\mu}/n$ is the same as the stationary solution for Θ appearing in (4). Moreover, though the derivation is slightly different, our formula (17) is exactly the same as the Heterogenous Mean Field method designed by Pastor-Satorras and Vespignani in [35]. HMF in the form above is an annealed method. It can easily be turned into a quenched method by using the actual degree frequencies.

The infection paradox leads to underestimation of μ/n , so the adaptation in (17) will increase our previous estimates (Heuristics 2a, 2b and 3) for the infected fraction. The same is true for the quenched version of HMF.

3.3.1 Mean-field methods NIMFA and HMF and size bias

NIMFA uses the full adjacency matrix, which means that degrees of neighbors are always counted correctly. NIMFA therefore does not make a systematic error caused by size bias. The same is true for HMF, which explicitly takes the size bias effect into account. This explains why both these methods give higher estimates for the infected fraction than for instance Heuristic 2a. This can be clearly seen in Figure 12. We simulated ER graphs with varying edge probability. For each p , 100 graphs were generated, and on each of them we

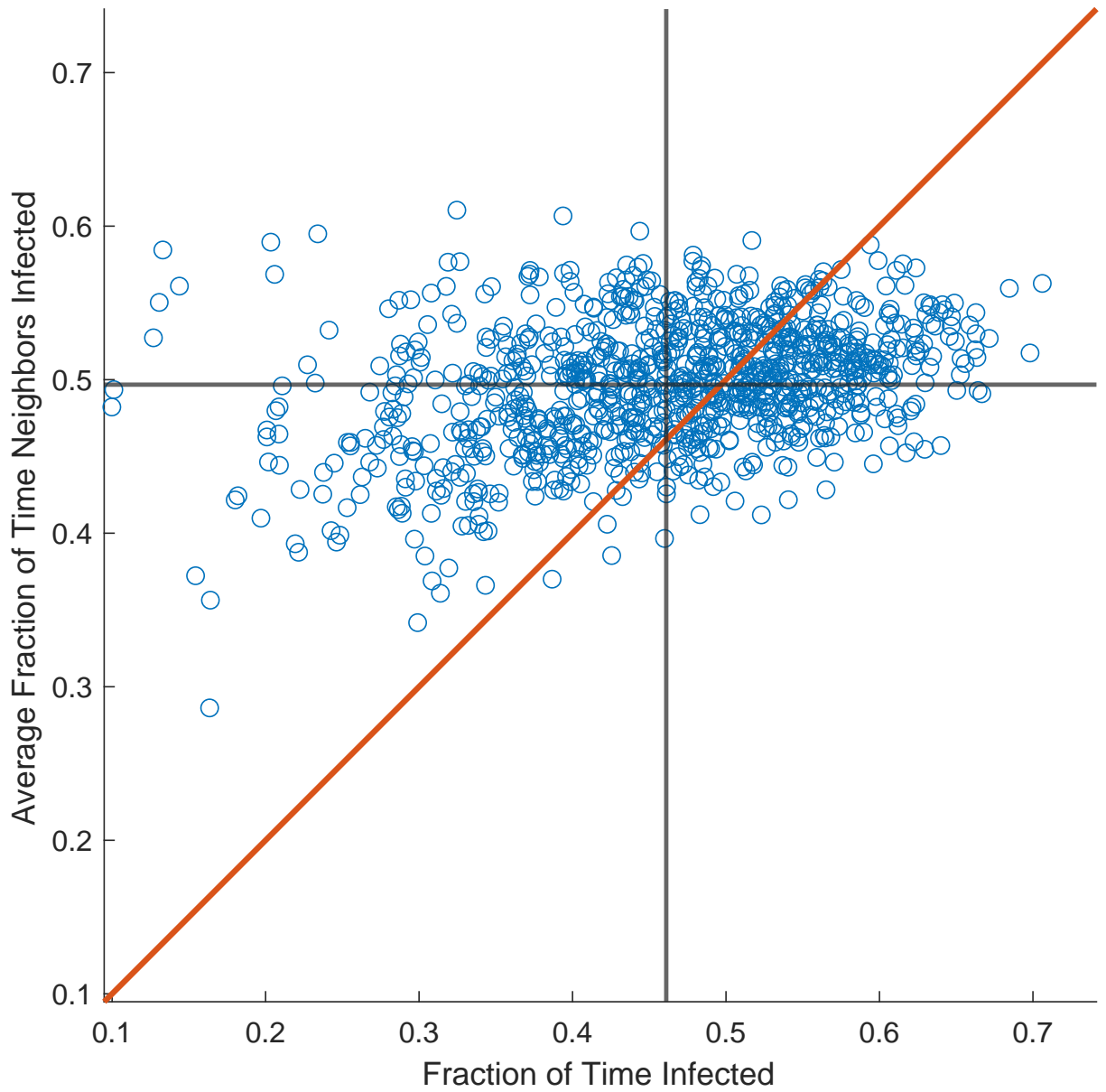


Figure 11: The infection paradox (ER graph with $n = 1000$, $p = \log(n)/n$, $\lambda = 2$): most nodes are less often infected than their neighbors. Averages are indicated by the horizontal and vertical line, they intersect clearly above the diagonal.

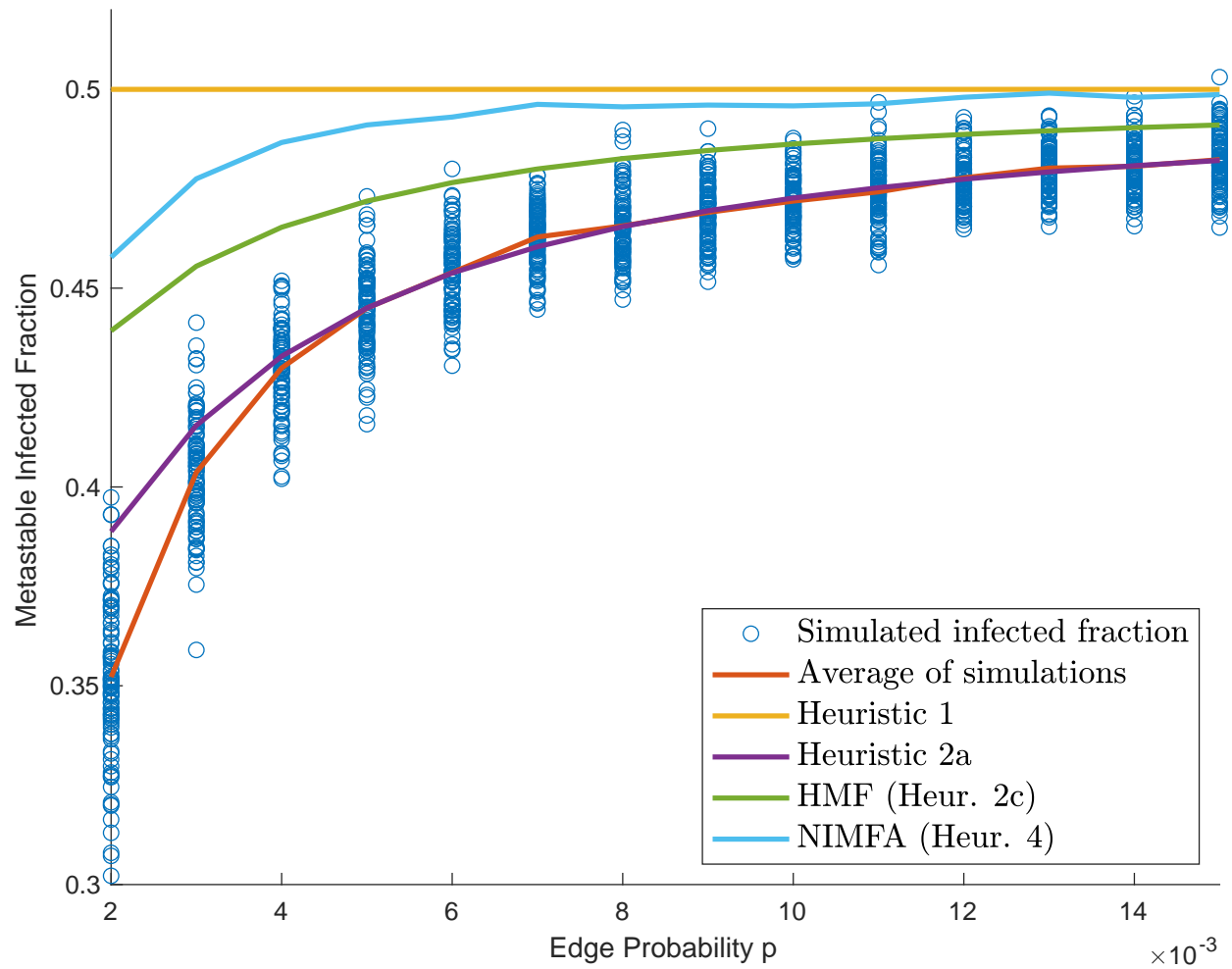


Figure 12: NIMFA and HMF systematically overestimate the infected fraction and are outperformed by Heuristic 2a. (ER graph, $n = 1000$, $\lambda = 2$)

simulated the SIS process. Again we see that Heuristic 1 is too simple, but 2a is much more accurate than HMF and NIMFA. Only when the graphs become really sparse with average degrees less than 5, Heuristic 2a visibly deviates from the simulation results. We will come back to this in Section 5.

By correcting for size bias, NIMFA and HMF actually become *more* biased than other methods. The reason is that there are two sources of systematic errors, which work in opposite directions and which often seem to almost cancel each other. The second error source is caused by correlations, and will be discussed in the next section. By repairing only one of these errors, NIMFA and HMF get their bias, which especially will be visible in sparse graphs.

3.4 Systematic errors II: neighbor correlation

So far we ignored dependence between neighboring nodes. For NIMFA, this is an explicit assumption. Also the other heuristics discussed before do not take dependence into account. Neighbors tend to align into the same state. When a node i is healthy, this increases the likelihood of its neighbors being healthy as well, see [11, 9]. By ignoring this, we overestimate the rate at which i gets infected by its neighbors. For this reason, the paper introducing NIMFA [43] already mentions that the method gives an upper bound for the infected fraction.

We illustrate the phenomenon of neighbor correlation in Figure 13. For each edge (i, j) in the graph, (co)variances are given by

$$\begin{aligned} \text{Cov}(X_i, X_j) &= \mathbb{E}(X_i X_j) - \mathbb{E}X_i \cdot \mathbb{E}X_j \\ &= \mathbb{P}(X_i = X_j = 1) - \mathbb{P}(X_i = 1) \cdot \mathbb{P}(X_j = 1). \end{aligned} \quad (18)$$

These are estimated by the corresponding simulated fractions of time, after which we can also estimate the correlation coefficients

$$\rho(X_i, X_j) = \frac{\text{Cov}(X_i, X_j)}{\sqrt{\text{Var}(X_i)\text{Var}(X_j)}}. \quad (19)$$

The figure plots the estimated correlation coefficients against the estimated product $\mathbb{P}(X_i = 1) \cdot \mathbb{P}(X_j = 1)$. Note that the correlation is weaker if the nodes are more often infected. A node which is frequently infected has more neighbors, so that the influence of an individual neighbor is less important.

All heuristics in the previous section use the assumption that the rate at which node i is infected by node j is equal to $\tau \cdot \mathbb{P}(X_j = 1)$. However, node j is only able to successfully infect i if i is healthy. Therefore, the actual rate at which j infects i is equal to $\tau \cdot \mathbb{P}(X_j = 1 \mid X_i = 0)$, which is smaller than $\tau \cdot \mathbb{P}(X_j = 1)$. In Figure 14, we see how the conditional probability $\mathbb{P}(X_j = 1 \mid X_i = 0)$ depends on the degree of i and the degree of j .

The left plot shows for each node i a simulated estimate of

$$\frac{1}{d_i} \sum_{j:i \sim j} \mathbb{P}(X_j = 1 \mid X_i = 0), \quad (20)$$

the average fraction of time its neighbors are infected, given that i itself is healthy (blue markers). The plot shows that this quantity only mildly depends on the degree of i . The variation in this average of conditional probabilities is mainly explained by the variation in the degrees of the *neighbors* of i . Taking for each node i the ratio

$$\frac{\sum_{j:i \sim j} \mathbb{P}(X_j = 1 \mid X_i = 0)}{\sum_{j:i \sim j} \mathbb{P}(X_j = 1)}, \quad (21)$$

we get very little variation (red markers). It therefore seems quite reasonable to base heuristics on the assumption that

$$\frac{1}{d_i} \sum_{j:i \sim j} \mathbb{P}(X_j = 1 \mid X_i = 0) \approx \frac{\eta}{d_i} \sum_{j:i \sim j} \mathbb{P}(X_j = 1) \quad (22)$$

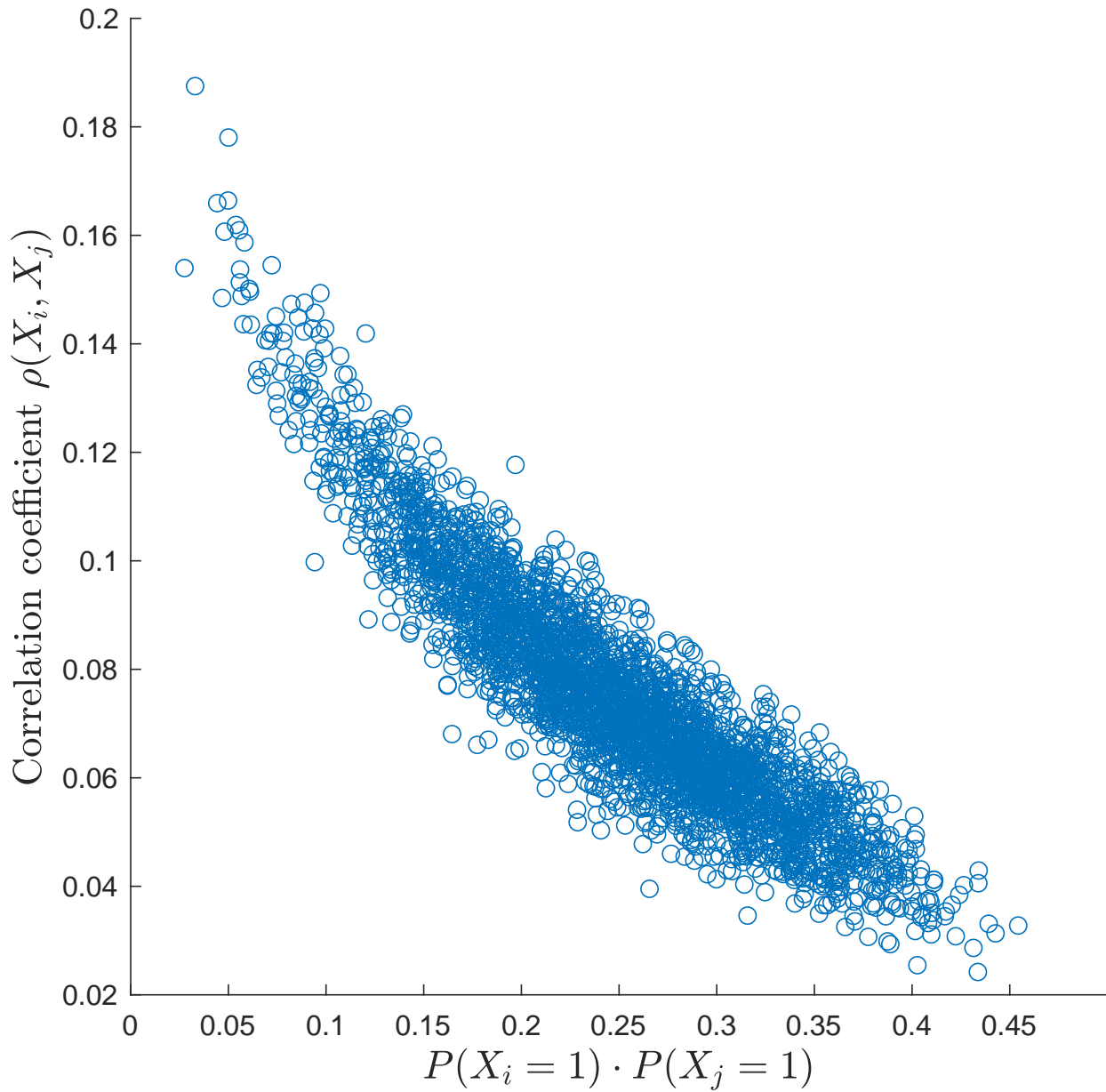


Figure 13: Neighbor correlations in Erdős-Rényi graph ($n = 1000$, $p = \log(n)/n$, $\lambda = 2$). Each marker represents an edge (i, j) .

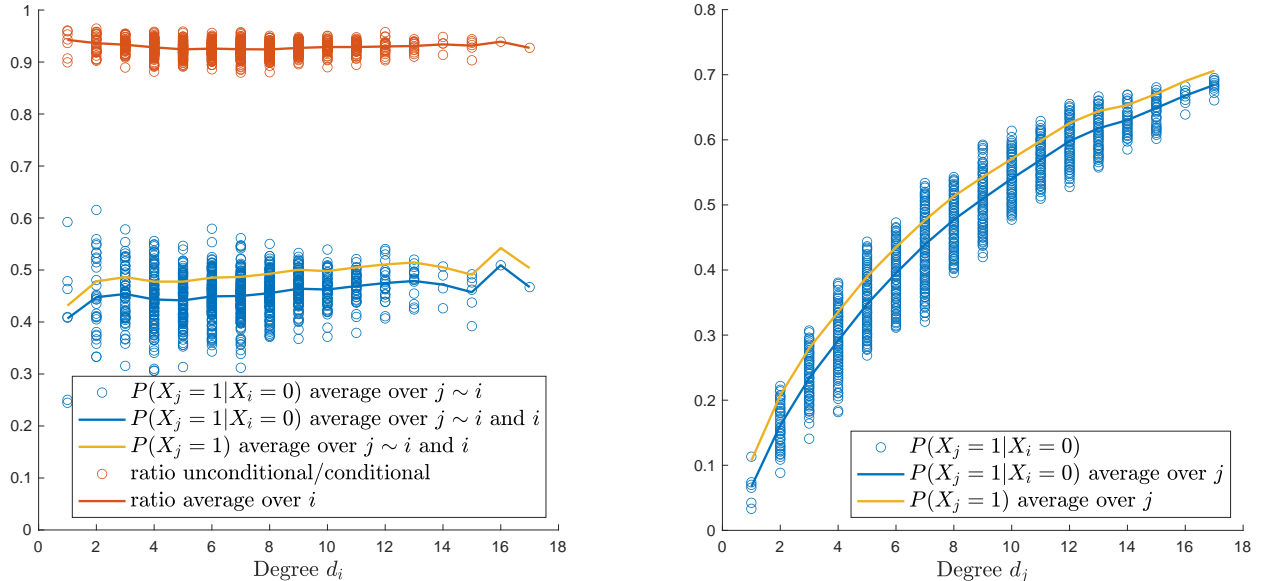


Figure 14: Dependence of conditional probabilities $\mathbb{P}(X_j = 1 | X_i = 0)$ on the degrees d_i and d_j . (ER graph $n = 1000$, $p = \log(n)/n$, $\lambda = 2$)

for some constant $0 < \eta < 1$ which does not depend on i and to try to estimate η . For each degree d , we also plotted the average of the conditional and of the unconditional probabilities,

$$\frac{1}{\#\{i : d_i = d\}} \sum_{i:d_i=d} \frac{1}{d} \sum_{j:i \sim j} \mathbb{P}(X_j = 1 | X_i = 0), \quad (23)$$

$$\frac{1}{\#\{i : d_i = d\}} \sum_{i:d_i=d} \frac{1}{d} \sum_{j:i \sim j} \mathbb{P}(X_j = 1), \quad (24)$$

and their ratio's (21) averaged over i (red). From the values on the yellow curve, we can reproduce an estimate of the size biased infected fraction $\tilde{\mu}/n$ by taking a weighted average:

$$\frac{\tilde{\mu}}{n} = \frac{1}{n} \sum_{d=1}^{n-1} \sum_{i:d_i=d} \frac{1}{d} \sum_{j:i \sim j} \mathbb{P}(X_j = 1). \quad (25)$$

Dependence of $\mathbb{P}(X_j = 1 | X_i = 0)$ on the degree of j is visible in the right plot of Figure 14. Each blue marker now corresponds to a single ordered edge (i, j) . Dependence of $\mathbb{P}(X_j = 1)$ on the degree of j has already been observed before, and here we see very similar patterns for the conditional probabilities $\mathbb{P}(X_j = 1 | X_i = 0)$. Averages of conditional and of unconditional probabilities are again given by the curves.

4 Taking size bias and neighbor correlations into account

The two types of systematic errors work in opposite directions. Ignoring the size bias effect leads to underestimation of the infected fraction μ/n of the population. On the other hand, ignoring correlation leads to overestimation of the infected fraction of the population.

The two errors might cancel sometimes, but in general this will not be the case, see for instance the smaller degrees in Figure 12. We therefore will propose heuristics to repair both errors. Nodes are still positively correlated if they are not direct neighbors. However, correlations rapidly decrease when the distance increases, Figure 15. Based on this observation, we will design a heuristic which takes correlations between direct neighbors into account, but ignores correlations between other pairs of nodes.

Consider random nodes i and j which are neighbors and have degrees $d_i \geq 1$ and $d_j \geq 1$. We make the following assumptions:

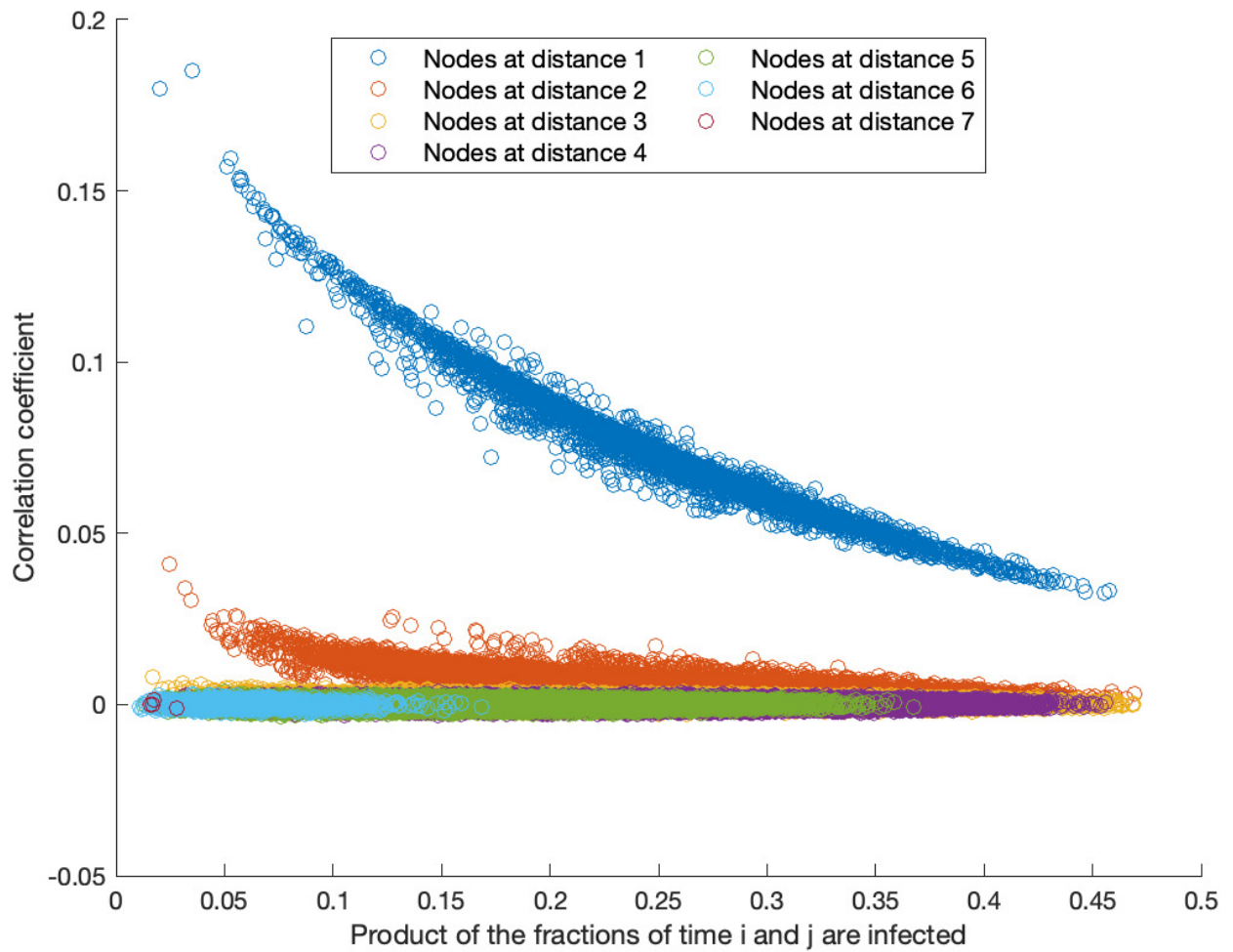


Figure 15: Correlations for each pair $\{i, j\}$ of nodes in an ER graph with $n = 1000$, $p = \log(n)/n$ and $\lambda = 2$. The color indicates the distance in the graph.

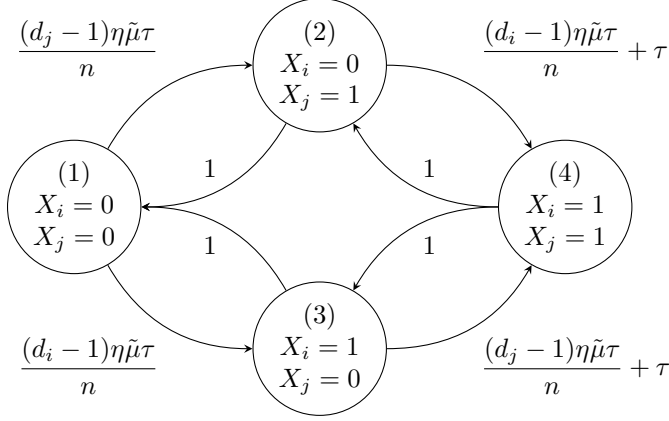


Figure 16: Transition diagram for infectious status of i and j . States are numbered (1), \dots , (4).

1. All neighbors of i and j (except i, j themselves) are infected the same fraction of time. We assume this fraction to be independent of d_i and d_j , and equal to the (unknown) size biased infected fraction $\tilde{\mu}/n$:

$$\mathbb{P}(X_k = 1) = \tilde{\mu}/n, \text{ for } k \sim i \text{ or } k \sim j, k \neq i, j.$$

2. All these neighbors are assumed to be independent of each other.
3. There exists a constant $\eta \in (0, 1)$ such that

$$\mathbb{P}(X_k = 1 \mid X_i = 0) = \eta\tilde{\mu}/n, \text{ for } k \sim i, k \neq j,$$

and similarly for i and j reversed.

Note that we do not use degrees other than the degrees of i and j . This causes the first assumption to be quite inaccurate for individual nodes, but it does keep the analysis feasible and the errors will mostly average out.

Under these assumptions, we are interested in the simultaneous evolution of nodes i and j . This evolution is described by a Markov chain on four states, with transition rates in the diagram in Figure 16.

This Markov chain has a unique stationary distribution, which is found by solving the equations (28) on page 26, where Q as given in (27) is the generator matrix.

The matrix Q has rank 3 and (28) has a unique solution, giving x_1, \dots, x_4 as functions of n, τ, d_i, d_j, η and $\tilde{\mu}$. In principle these functions can be determined exactly. We will not do this, but we will show that in this system X_i and X_j have positive correlation, which vanishes if the degrees go to infinity. This agrees with conjectured and simulated behaviour of the SIS process.

First we take a look at the Markov chain for $np \rightarrow \infty$. In this case, by the law of large numbers, $(d_i - 1)/(np) \rightarrow 1$ and $(d_j - 1)/(np) \rightarrow 1$ as $n \rightarrow \infty$. Since $\tau = \lambda/(np)$ is of order $(np)^{-1}$, all rates to the right are of constant order and asymptotically equal to $\lambda\eta\tilde{\mu}/n$. By symmetry, states (2) and (3) will then have the same stationary probability. The Markov chain therefore asymptotically simplifies to the one in Figure 18. Solving for the stationary distribution of this system, we can easily find \mathbf{x} as well:

$$\mathbf{x}^T = \frac{1}{(1+c)^2} \cdot (1, c, c, c^2), \quad \text{where } c = \frac{\lambda\eta\tilde{\mu}}{n}. \quad (31)$$

We note that from this solution it follows that nodes i and j become independent as the degrees go to ∞ :

$$\begin{aligned} \mathbb{P}(X_i = 0) \cdot \mathbb{P}(X_j = 0) &= (x_1 + x_2)(x_1 + x_3) \\ &= \left(\frac{1+c}{(1+c)^2} \right)^2 = \mathbb{P}(X_i = X_j = 0). \end{aligned} \quad (32)$$

Now consider the more complicated Markov chain of Figure 16. To avoid very awkward calculations, define

Given: a connected graph $G = (V, E)$ with $V = \{1, \dots, n\}$. Infection rate: τ . Healing rate: 1.

1. Compute

$$P(d) := \frac{\#\{i \in V : \deg(i) = d\}}{n}, \quad \tilde{P}(d) = \frac{d \cdot \#\{i \in V : \deg(i) = d\}}{\sum_i d_i}. \quad (26)$$

2. For each pair of degrees (d_i, d_j) , define a matrix $Q := Q(\eta, \tilde{\mu})$ by

$$Q = \begin{pmatrix} -\sum_{\ell \neq 1} Q_{1,\ell} & (d_j - 1)\eta\tilde{\mu}\tau/n & (d_i - 1)\eta\tilde{\mu}\tau/n & 0 \\ 1 & -\sum_{\ell \neq 2} Q_{2,\ell} & 0 & ((d_i - 1)\eta\tilde{\mu}\tau/n) + \tau \\ 1 & 0 & -\sum_{\ell \neq 3} Q_{3,\ell} & ((d_j - 1)\eta\tilde{\mu}\tau/n) + \tau \\ 0 & 1 & 1 & -\sum_{\ell \neq 4} Q_{4,\ell} \end{pmatrix}, \quad (27)$$

and determine the solution $\mathbf{x} = \mathbf{x}(d_i, d_j)$ (as function of η and $\tilde{\mu}$) of

$$\begin{cases} \mathbf{x}^T Q = \mathbf{0}^T, \\ \mathbf{x}^T \mathbf{1} = 1, \end{cases} \quad \mathbf{x}^T = (x_1 \quad x_2 \quad x_3 \quad x_4), \quad (28)$$

where $\mathbf{0}$ and $\mathbf{1}$ are the all zero and all one vector in \mathbb{R}^4 .

3. Determine η and $\tilde{\mu}$ by solving the equations

$$\frac{\tilde{\mu}}{n} = \sum_{d_i} \sum_{d_j} P(d_i) \tilde{P}(d_j) (x_2(d_i, d_j) + x_4(d_i, d_j)), \quad \frac{\eta\tilde{\mu}}{n} = \sum_{d_i} \sum_{d_j} P(d_i) \tilde{P}(d_j) \frac{x_2(d_i, d_j)}{x_1(d_i, d_j) + x_2(d_i, d_j)}. \quad (29)$$

4. Estimate the infected fraction by

$$\frac{\mu}{n} = \sum_{d_i} \sum_{d_j} P(d_i) \tilde{P}(d_j) (x_3(d_i, d_j) + x_4(d_i, d_j)). \quad (30)$$

Figure 17: Main result: Algorithm (quenched) to estimate the metastable infected fraction in a connected graph G with n nodes.

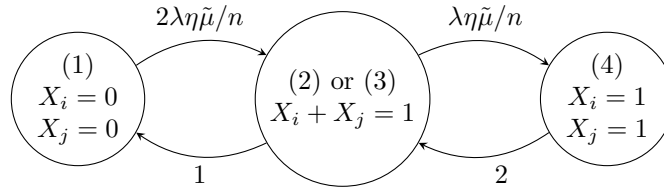


Figure 18: Transition diagram for infectious status of i and j as $np \rightarrow \infty$

$$a = \frac{(d_i - 1)\eta\tilde{\mu}\tau}{n}, \quad b = \frac{(d_j - 1)\eta\tilde{\mu}\tau}{n}. \quad (33)$$

Since $\tau > 0$, the rate from $X_i = 0$ to $X_i = 1$ is at least a . Therefore,

$$\mathbb{P}(X_i = 0) < \frac{1}{1+a}, \quad \mathbb{P}(X_j = 0) < \frac{1}{1+b},$$

so that in particular there exist constants $r_1, r_2 < 1$ for which $x_1 + x_2 = r_1/(1+a)$ and $x_1 + x_3 = r_2/(1+b)$. Further, the detailed balance equation for state (1) yields $(a+b)x_1 = x_2 + x_3$, and hence

$$(2+a+b)x_1 = 2x_1 + x_2 + x_3 = \frac{r_1}{1+a} + \frac{r_2}{1+b}. \quad (34)$$

Solving this for $x_1 = \mathbb{P}(X_i = X_j = 0)$, we obtain

$$\begin{aligned} \mathbb{P}(X_i = X_j = 0) &= \frac{r_1(1+b) + r_2(1+a)}{(1+a)(1+b)(2+a+b)} \\ &> \frac{r_1 r_2}{(1+a)(1+b)} = \mathbb{P}(X_i = 0) \cdot \mathbb{P}(X_j = 0), \end{aligned} \quad (35)$$

proving positive correlation for all choices of the parameters.

As noted, given the parameters n, τ, d_i, d_j , we can determine the solution \mathbf{x} . However, this solution will still depend on the unknown η and $\tilde{\mu}$. To solve for these variables, we need additional equations.

So far, i and j have played the same role. But now we consider j to be a random neighbor of a randomly chosen node i . This is only possible if i has degree at least 1. In a connected graph, this is automatic. In an Erdős-Rényi graph with small p , it means that d_i has distribution $\text{Bin}(n-1, p)$, conditioned on being non-zero. Node j has the size biased degree distribution $d_j - 1 \sim \text{Bin}(n-2, p)$, which is non-zero by definition. Consequently, j has the same degree distribution as all neighbors of i and j (except i itself). It therefore makes sense to approximate the expected fraction of time j is infected by the same $\tilde{\mu}/n$. Concretely, for each combination of d_i and d_j , we solve the system (28) for $\mathbf{x} = \mathbf{x}(d_i, d_j)$. In particular we get a different solution

$$\mathbb{P}(X_j = 1) = x_2(d_i, d_j) + x_4(d_i, d_j)$$

for each combination (d_i, d_j) . Then we take a weighted average according to the degree distributions of i and j . The resulting equation is

$$\frac{\tilde{\mu}}{n} = \sum_{d_i=1}^{n-1} \sum_{d_j=1}^{n-1} P^{(\geq 1)}(d_i) \tilde{P}(d_j) (x_2 + x_4), \quad (36)$$

where $P^{(\geq 1)}(d_i)$ and $\tilde{P}(d_j)$ are the probabilities that i and j have degrees d_i and d_j respectively. That is,

$$\begin{aligned} P^{(\geq 1)}(d_i) &= \mathbb{P}(D = d_i \mid D \geq 1), & D &\sim \text{Bin}(n-1, p), \\ \tilde{P}(d_j) &= \mathbb{P}(\tilde{D} = d_j), & \tilde{D} &\sim 1 + \text{Bin}(n-2, p). \end{aligned}$$

Of course these probabilities can be replaced by suitable approximations for large n or by graph-based estimates (see Section 5).

Another equation is obtained by considering conditional probabilities. Since $\mathbb{P}(X_j = 1 \mid X_i = 0)$ hardly depends on the degree of i (supported by Figure 14), we can assume this conditional probability to be equal to $\eta\tilde{\mu}$. In terms of \mathbf{x} , we have

$$\mathbb{P}(X_j = 1 \mid X_i = 0) = \frac{x_2}{x_1 + x_2}.$$

Proceeding along the same lines as above, we obtain

$$\frac{\eta\tilde{\mu}}{n} = \sum_{d_i=1}^{n-1} \sum_{d_j=1}^{n-1} P^{(\geq 1)}(d_i) \tilde{P}(d_j) \frac{x_2}{x_1 + x_2}. \quad (37)$$

If all parameters of the process are given, the equations (28), (36) and (37) can be solved to find η and $\tilde{\mu}$. Finding exact expressions is a tall order, but an iterative numerical procedure gives satisfactory results.

The solutions for η and $\tilde{\mu}$ only depend (in a complicated way) on the process parameters n , p and τ . Once they have been determined, we can plug them into \mathbf{x} , which will then be a function of the same parameters and the degrees d_i and d_j . This allows to compute an estimate for μ in the same fashion, by using that $\mathbb{P}(X_i = 1) = x_3 + x_4$ and taking a weighted average similar to (36). This time, we first pick a random node i . If it has degree 0, it will not contribute to μ (it quickly heals and never gets infected again). If it has degree ≥ 1 , we let j be a random neighbor of i . The estimate for μ then is

$$\frac{\mu}{n} = \sum_{d_i=1}^{n-1} \sum_{d_j=1}^{n-1} P(d_i) \tilde{P}(d_j) (x_3 + x_4), \quad (38)$$

with

$$P(d_i) = \mathbb{P}(D = d_i), \quad D \sim \text{Bin}(n-1, p). \quad (39)$$

The subtle difference with (36) and (37) is that now i is not conditioned to have degree ≥ 1 , though still degree 0 does not contribute to the sum.

The resulting equations for $\tilde{\mu}$ and μ can be seen as a more sophisticated version of the Heterogeneous Mean Field method ((16) and (17)). It takes size bias effects and correlations simultaneously into account. We now obtain a new annealed heuristic for estimating μ as a function of n , p and τ :

Heuristic 5 (Annealed). *Let $G = (V, E)$ be an Erdős-Rényi graph with parameters n and p . Consider the SIS process on G with infection rate τ . For each $1 \leq d_i, d_j \leq n-1$, let $\mathbf{x}(d_i, d_j)$ be the solution of (28), which depends on the unknowns $\tilde{\mu}$ and η . Solve (36) and (37) for $\tilde{\mu}$ and η and substitute the solutions in $\mathbf{x}(d_i, d_j)$. Finally, take the weighted average (38) to obtain an estimate for μ .*

This heuristic can easily be generalized to any connected graph, given its degree sequence (Figure 17).

Before turning to the numerical results, we wrap up our discussion on asymptotics for $np \rightarrow \infty$. The degree distributions of d_i and d_j concentrate around their expectations, and \mathbf{x} becomes independent of the degrees as in (31). The equations (36) and (37) become

$$\frac{\tilde{\mu}}{n} = x_2 + x_4 = \frac{c + c^2}{(1+c)^2} = \frac{c}{1+c} \quad (40)$$

$$\frac{\eta \tilde{\mu}}{n} = \frac{x_2}{x_1 + x_2} = \frac{c/(1+c)^2}{(1+c)/(1+c)^2} = \frac{c}{1+c}, \quad (41)$$

and solving them gives

$$\tilde{\mu} = (1 - \lambda^{-1})n, \quad \eta = 1. \quad (42)$$

Since $x_2 = x_3$ in this case, we also get $\mu = \tilde{\mu}$. The conclusion is that according to Heuristic 5, both the size bias effect and the correlations vanish if the degrees go to infinity. This conclusion is consistent with simulations and intuition. Also note that the asymptotic estimate for μ agrees with Heuristic 1, which can be seen as a small sanity check. Finally, no solution exists for $\lambda < 1$, reflecting the fact that the process has no metastable behaviour in this case.

4.1 Quenched variants

Heuristic 5 can be reinforced if information about the graph is available. In particular, we can replace $P(d)$, $P^{(\geq 1)}(d)$ and $\tilde{P}(d)$ with graph-based estimates. We only have to do this for $d \geq 1$. We have the following quenched variants of Heuristic 5:

Heuristic 5 (Quenched variants). (a) *Estimate p by the number of edges m in the graph: $\hat{p} = \frac{2m}{n(n-1)}$.*

(b) Estimate probabilities by true degree frequencies in the graph:

$$\begin{aligned}
 P(d) &= \frac{\#\{i : d_i = d\}}{n} = \frac{1}{n} \sum_{i=1}^n \mathbf{1}\{d_i = d\}, \\
 P^{(\geq 1)}(d) &= \frac{\#\{i : d_i = d\}}{\#\{i : d_i \geq 1\}} = \frac{\sum_{i=1}^n \mathbf{1}\{d_i = d\}}{\sum_{i=1}^n \mathbf{1}\{d_i \geq 1\}}, \\
 \tilde{P}(d) &= \frac{1}{\#\{i : d_i \geq 1\}} \sum_{i=1, d_i \geq 1}^n \frac{1}{d_i} \sum_{j \sim i} \mathbf{1}\{d_j = d\}.
 \end{aligned}$$

(c) Estimate products of probabilities by true frequencies in the graph:

$$\begin{aligned}
 P(d) \cdot \tilde{P}(e) &= \frac{1}{n} \sum_{i=1}^n \sum_{j \sim i} \frac{\mathbf{1}\{d_i = d, d_j = e\}}{d}, \\
 P^{(\geq 1)}(d) \cdot \tilde{P}(e) &= \frac{1}{\#\{i : d_i \geq 1\}} \sum_{i=1}^n \sum_{j \sim i} \frac{\mathbf{1}\{d_i = d, d_j = e\}}{d}.
 \end{aligned}$$

As in NIMFA, one could even use the full adjacency matrix of the graph, but computations would be more complicated.

5 Heuristic 5, numerical results

In this section we review the performance of annealed and quenched variants of Heuristic 5. For p equal to the connectivity threshold $\log(n)/n$, Heuristics 2 and 3 are already very good (Figures 9 and 10). Nevertheless, Heuristic 5 seems to give a small improvement here. We will not discuss this in detail.

The real test case is the very sparse Erdős-Rényi graph with p significantly below the connectivity threshold. In this case all heuristics which do not take into account correlations fail to accurately estimate. This is the case for NIMFA and HMF, but in this sparse regime it also applies to Heuristics 2 and 3. We will demonstrate how Heuristic 5 can be used to get accurate estimations in this regime (Section 5.1).

Heuristic 5 does not only give accurate estimates for the infected fraction of the population. As a bonus, it can also be exploited to obtain estimates for other quantities like correlations between nodes (Section 5.2).

5.1 Estimation in sparse graphs, the regime $p = c/n$

The effect of correlations and size bias becomes more important when degrees in the graph are smaller. So far we mostly looked at Erdős-Rényi graphs with p close to or above the connectivity threshold. In these cases, variants of Heuristic 2 still do reasonably well. Below the connectivity threshold, the picture changes.

In the left plot of Figure 19, we compare all annealed heuristics for Erdős-Rényi graphs with $p = c/n$ and the average degree c ranging from 1.1 to 7 ($\approx \log(n)$). For each parameter combination and heuristic, an average of simulations is compared with the corresponding estimates. In the plot on the right, we zoom in on the errors for 100 replications of the case $c = 2$.

For $p = c/n$, $c > 1$, the graph disconnects and there will be a unique giant component. This giant component has size about $y \cdot n$, with y the largest solution of $1 - y = e^{-cy}$, see [41]. All other components will be much smaller, of size at most logarithmic in n . In these small components the infection quickly disappears. The metastable infected fraction of the population therefore will be less than the size of the giant component. The simulation in Figure 19 confirms this, but none of the heuristics captures this effect.

Our implementations of Heuristic 5 so far do not account for these properties of subcritical Erdős-Rényi graphs. For the degree distribution they just take the binomials which apply to the whole graph. However, for small c , one should restrict the analysis to the giant and use the corresponding degree distributions. The degree distributions in the entire graph, in the giant component and their size biased versions are all different in the sparse regime. Only when the degrees go to infinity, these differences will be negligible. The calculation of these distributions is elementary. Heuristic 5 can then be used to estimate the infected fraction

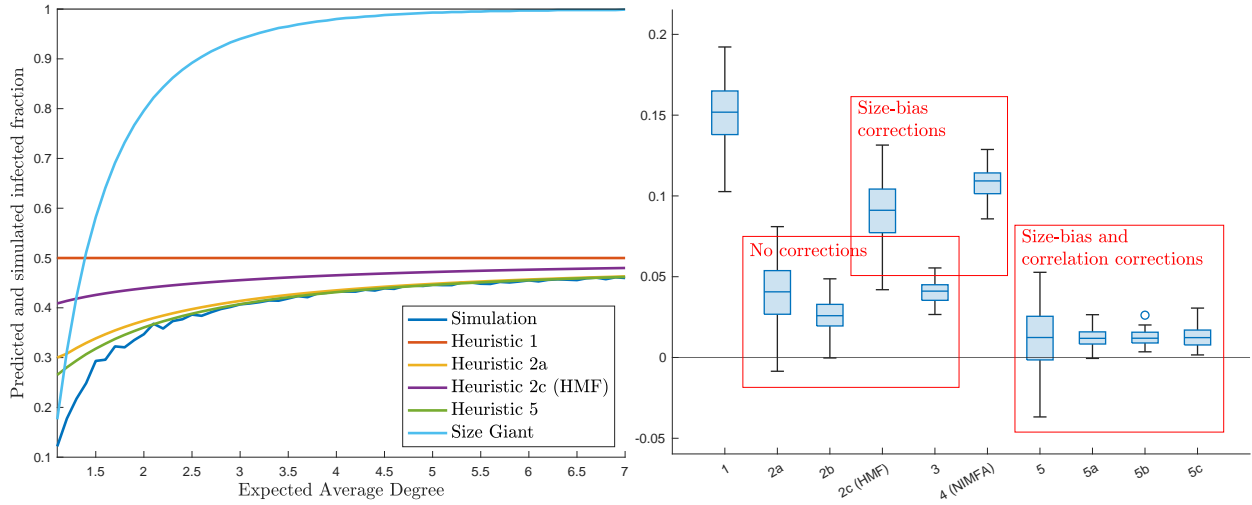


Figure 19: Sparse Erdős-Rényi graphs ($n = 1000$, $\lambda = 2$). Left: simulation compared to annealed heuristics. Right: estimation errors for all heuristics in Erdős-Rényi graphs with expected average degree $np = 2$.

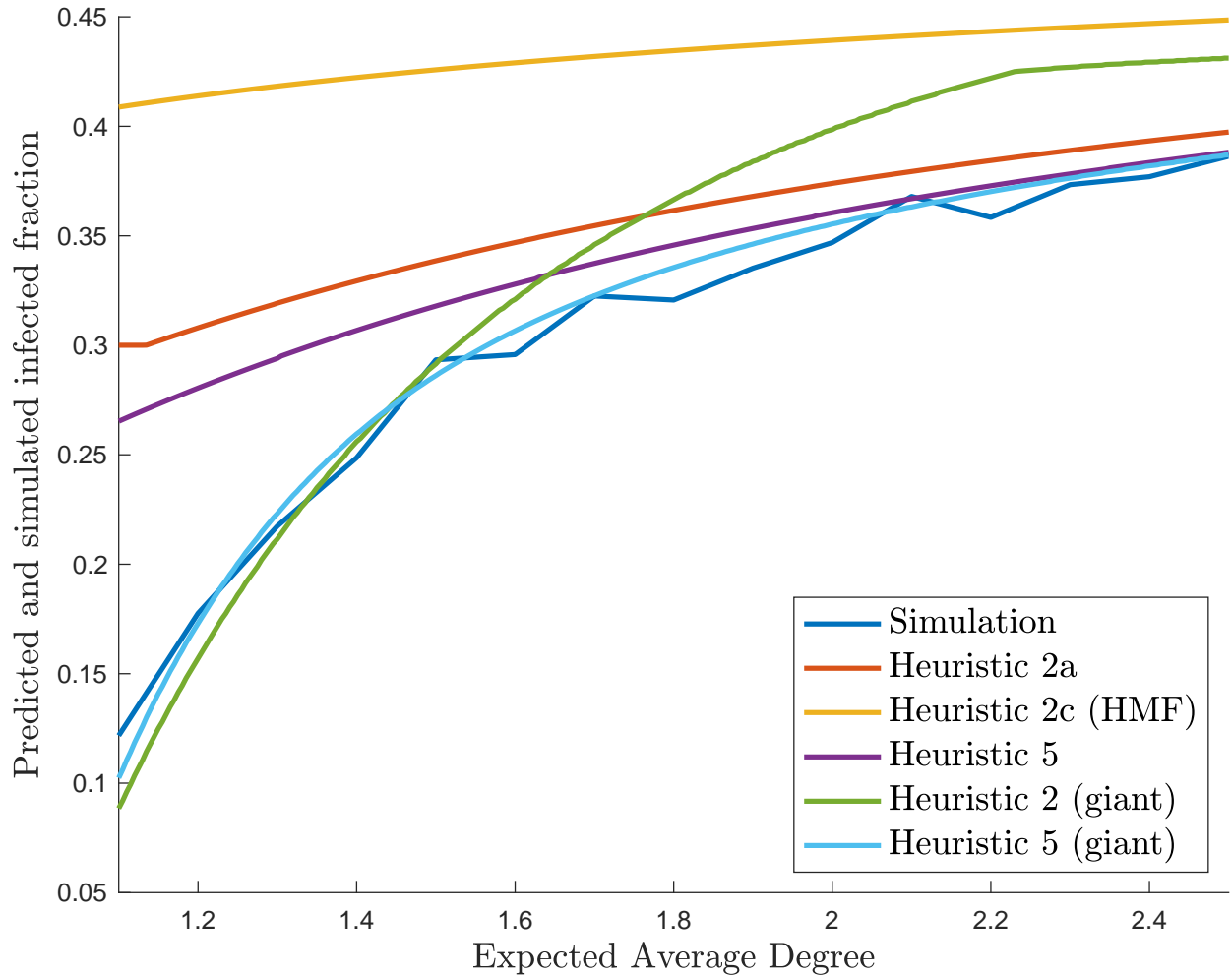


Figure 20: Most heuristics are wrong in very sparse Erdős-Rényi graphs ($n = 1000$, $\lambda = 2$). One should take the degree distribution of the giant component and apply size bias and correlation corrections (light blue).

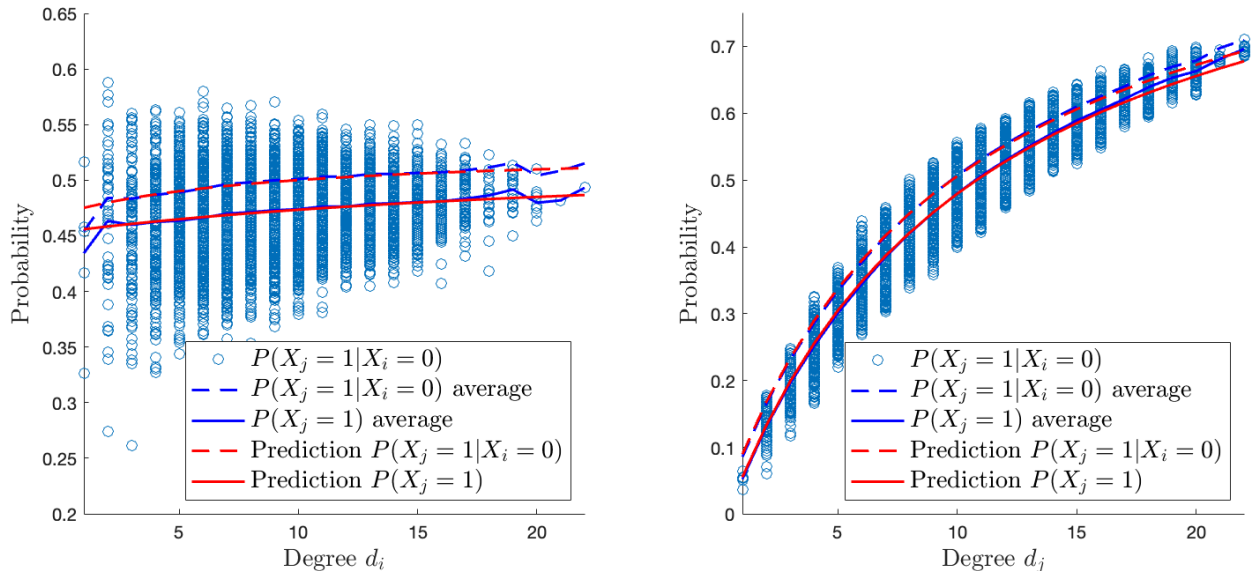


Figure 21: Infection probabilities and conditional infection probabilities for pairs (i, j) with estimates (ER graph $n = 10^4$, $p = \log(n)/n$, $\lambda = 2$). Left: averaged over neighbors of i and as function of d_i . Right: as function of d_j .

within the giant component. After rescaling by the expected size of the giant component, we obtain annealed estimates for μ/n in the Erdős-Renyi graph. Note that this procedure still only uses the parameters, no graph information is needed.

Figure 20 shows that this gives pretty accurate results (see also the red curves in Figure 4). It also shows that it is insufficient to merely use the correct degree distributions for the giant, apply Heuristic 2 and then rescale by the size of the giant component. Correlations and size bias have to be taken into account as well.

In a similar fashion quenched heuristics can be applied to the giant component. An illustration is given in Figure 4, where the quenched method only uses the sum of the degrees as in Heuristic 5a (so not the actual degrees, not the actual size of the giant component). These quenched versions also turn out to give very accurate estimates.

The analysis of the giant component serves as a test case for graphs with other degree distributions. Since our methods work quite well in the giant component, we expect them to apply to graphs with other degree distributions as well. Which features of the graph are essential to make the methods work requires further research. We expect that the methods are less suitable for graphs with a high variation in degrees (like power-law degree distributions) and for graphs which locally do not look like a tree (like grids). Graphs for which we do expect good results include the random regular graph.

5.2 Estimating per-node infected fractions, correlations and the total variance

The ideas behind Heuristic 5 give more information than just an estimate for μ . After solving all equations, we know $\mathbf{x}(d_i, d_j)$ for all combinations of d_i and d_j . This means that we can make degree-dependent estimates. For instance, to estimate the fraction of time a random node of degree d is infected, take $d_i = d$ and average over d_j (cf. (38)). Similarly, we can estimate conditional probabilities.

For illustration, see Figure 21. The simulation is essentially the same as Figure 14, but now we can estimate these quantities as follows. Let i and j be neighboring nodes. First we solve for $\mathbf{x}(d_i, d_j)$ as in Heuristic 5. An approximation for $\mathbb{P}(X_j = 1 | X_i = 0)$ is $x_2/(x_1 + x_2)$. Fixing d_i and taking a weighted average over all values of d_j gives an estimate for $\mathbb{P}(X_j = 1 | X_i = 0)$ as function of d_i . Similarly, we get estimates as function of d_j . These estimates are as in (37), but now only summing over d_j or only over d_i respectively. For the unconditional probabilities $\mathbb{P}(X_j = 1)$, the procedure is analogous, but now using (36). In fact, by looking at pairs, we are estimating a version of a size biased distribution here. Similar methods

can be used to estimate the infected fraction of time for a random node with degree d_i using (38) and only summing over d_j .

Another feature of interest are correlations between neighbors. For an edge (i, j) with degrees d_i and d_j , we can solve for $\mathbf{x}(d_i, d_j)$, estimate the (co)variances cf. (18) by

$$\begin{aligned}\text{Cov}(X_i, X_j) &= x_4 - (x_3 + x_4) \cdot (x_2 + x_4), \\ \text{Var}(X_i) &= (x_3 + x_4)(1 - (x_3 + x_4)), \\ \text{Var}(X_j) &= (x_2 + x_4)(1 - (x_2 + x_4)),\end{aligned}\tag{43}$$

and then the correlation coefficient $\rho(X_i, X_j)$ of i and j by (19). Plotting this against

$$\mathbb{P}(X_i = 1) \cdot \mathbb{P}(X_j = 1) \approx (x_3 + x_4) \cdot (x_2 + x_4)\tag{44}$$

gives Figure 22. The left hand sides of (43) and (44) are simulated, the right hand sides are estimations. For each combination of degrees d_i and d_j , there is one estimated point, plotted as a red marker. The size of the marker is proportional to the probability of the degree pair (d_i, d_j) . We see that correlations are maybe slightly underestimated for the less likely degree combinations. This could be explained by the fact that Heuristic 5 ignores correlations at distance 2 and larger.

One could wonder if we can use these correlation estimates to obtain estimates for the variance of the number of infected nodes. We have

$$\text{Var}\left(\sum_{i=1}^n X_i\right) = \sum_{i=1}^n \text{Var}(X_i) + 2 \sum_{i \neq j} \text{Cov}(X_i, X_j).\tag{45}$$

For instance, in the complete graph expectation and variances are known:

$$\begin{aligned}\mathbb{E}[X_i] &= 1 - \frac{1}{\lambda}, \text{Var}(X_i) = \frac{1}{\lambda}\left(1 - \frac{1}{\lambda}\right), \\ \text{Var}\left(\sum X_i\right) &= \frac{n}{\lambda}.\end{aligned}$$

Substituting in (45) gives

$$n\lambda^{-1} = n\lambda^{-1}(1 - \lambda^{-1}) + n(n-1)\text{Cov}(X_1, X_2),\tag{46}$$

So we can compute the covariances as well to find $\text{Cov}(X_1, X_2) \sim 1/(n\lambda^2)$. This means that pair covariances are small compared to node variances, but the sum of covariances significantly contributes to the total variance.

In the Erdős-Rényi graph, we can estimate $\mu = \sum \mathbb{E}[X_i]$ as in (38). Similarly, we estimate the sum of variances

$$\sum_i \text{Var}(X_i) = \sum_i \mathbb{E}[X_i^2] - \mathbb{E}[X_i]^2$$

by taking a weighted average of degree-dependent estimates.

For covariances of neighbors, we have degree-dependent estimates $\text{Cov}(d_i, d_j)$ as well in (43). This can be used to estimate $2 \sum_{i \sim j} \text{Cov}(X_i, X_j)$ by

$$pn(n-1) \sum_{d_i=1}^{n-1} \sum_{d_j=1}^{n-1} \tilde{P}(d_i) \tilde{P}(d_j) \text{Cov}(d_i, d_j).\tag{47}$$

This is twice the expected number of edges, multiplied by the estimated covariance for a randomly chosen edge. A subtlety to be noted here is the weighting: if we pick a random edge, then both endpoints have the size biased degree distribution.

What is still missing to estimate the total variance in (45) are covariances for pairs of non-neighboring nodes. Figure 23 shows simulations and estimates for the terms

$$\sum_i \text{Var}(X_i), \quad 2 \sum_{i \sim j} \text{Cov}(X_i, X_j).\tag{48}$$

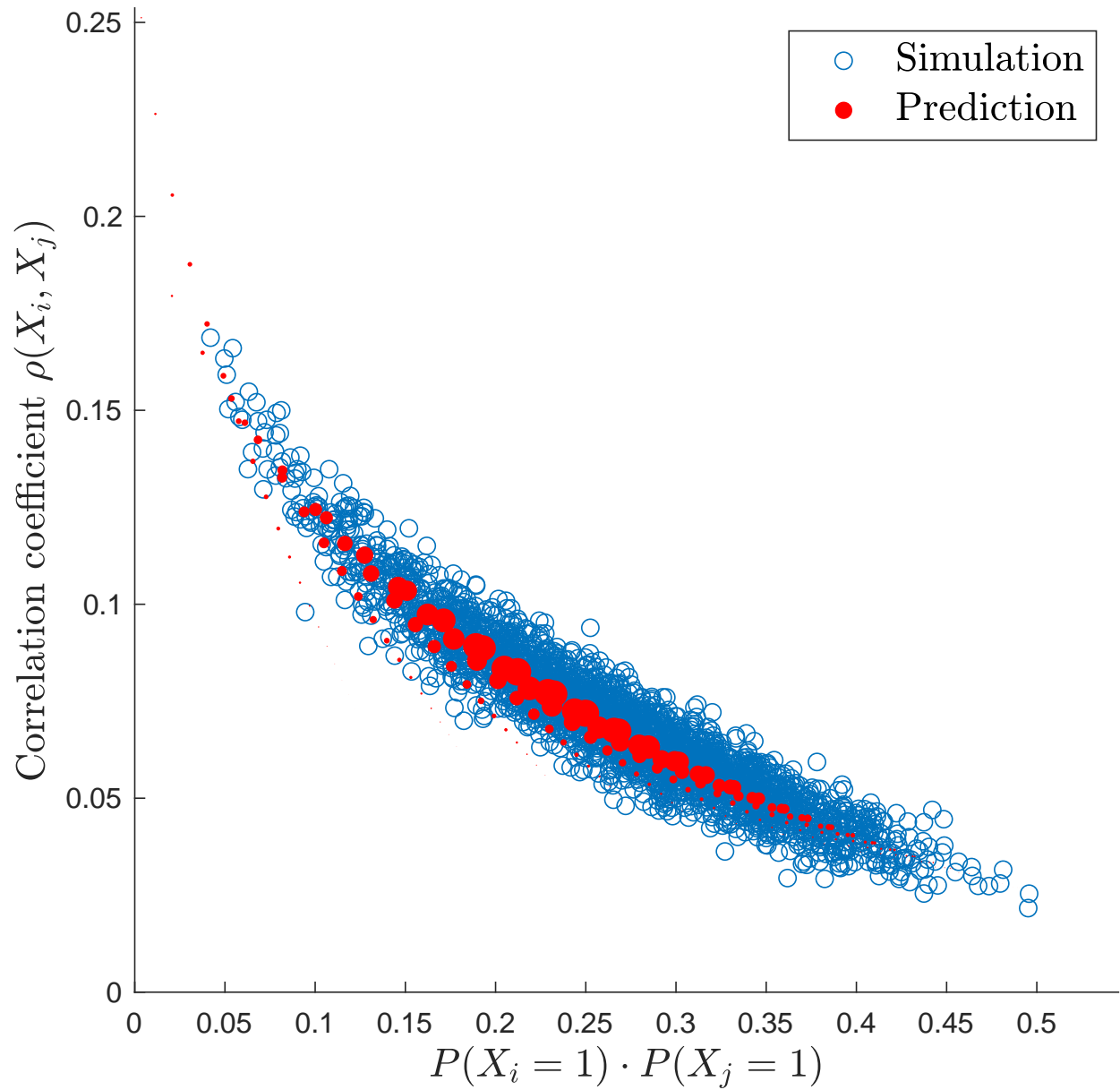


Figure 22: Simulated and estimated correlations. (ER graph $n = 10^4$, $p = \log(n)/n$, $\lambda = 2$)

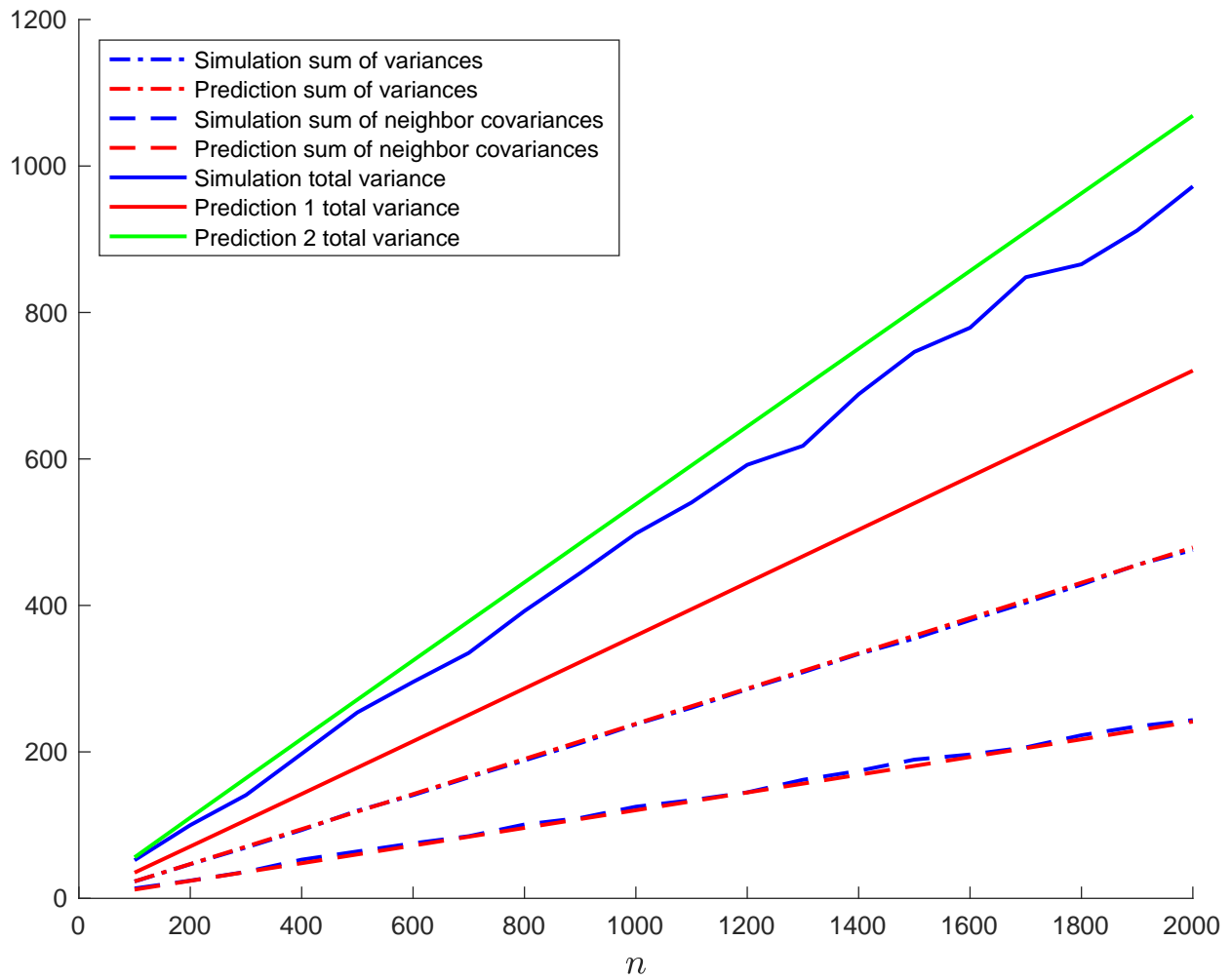


Figure 23: Simulations and estimates of variances and covariances. (ER graph $p = \log(n)/n$, $\lambda = 2$)

Both terms are estimated quite accurately. However, the sum of these two (solid red in the figure) turns out to be a bad estimate for the total variance, which was simulated as well. This means that we can not ignore correlations between nodes at mutual distance 2 or larger. The covariances $\text{Cov}(X_i, X_j)$ for $i \not\sim j$ are much smaller (cf. Figure 15), but the number of pairs is much larger, making the sum a significant contribution to the total variance. Since Heuristic 5 is based on analysis of direct neighbors, it falls short to estimate the total variance.

There is however another way to estimate the total variance. In equilibrium, the total healing rate is equal to μn . By definition of equilibrium, this is equal to the total infection rate. For a uniformly at random selected set of μn nodes, we expect $p\mu(1-\mu)n^2$ edges to its complement. The set of infected nodes is *not* a uniform selection (e.g. high degrees are overrepresented). Still, if the number of infected k is close to equilibrium, we can assume that the number of edges to the complement is proportional $k(n-k)$. In equilibrium ($k = \mu n$), the total infection rate is $\tilde{p}\tau\mu(1-\mu)n^2$, where \tilde{p} is a conditional edge probability given that we consider a healthy and an infected node. This gives the equilibrium equation

$$\mu n = \tilde{p}\tau\mu(1-\mu)n^2, \quad (49)$$

so that $\tilde{p}\tau$ is equal to the reciprocal of the number $(1-\mu)n$ of healthy nodes in equilibrium. Note that this is consistent with the complete graph, when $p = \tilde{p} = 1$.

Now suppose the number of infected deviates a bit from equilibrium and is equal to $k = \mu n + d$. The ratio of total infection and total healing rate is then given by

$$\frac{\tilde{p}\tau(\mu n + d)((1-\mu)n - d)}{\mu n + d} = 1 - \frac{d}{(1-\mu)n}. \quad (50)$$

In this formula, we see a drift towards the equilibrium μn . This type of drift is known to lead to a Gaussian metastable distribution with variance $(1-\mu)n$, see [3]. Since we have an estimate for μ , we have an estimate for the variance as well, which is added to the plot in Figure 23 (solid green). This improves the estimate based on Heuristic 5, but is still biased. A better understanding of correlations of non-neighboring nodes will be needed to get more accurate variance estimates.

References

- [1] Massimo A Achterberg, Bastian Prasse, and Piet Van Mieghem. Analysis of continuous-time markovian ε -SIS epidemics on networks. *Physical Review E*, 105(5):054305, 2022.
- [2] Erik Aurell, Gino Del Ferraro, Eduardo Domínguez, and Roberto Mulet. Cavity master equation for the continuous time dynamics of discrete-spin models. *Physical Review E*, 95(5):052119, 2017.
- [3] O. S. Awolude, E. Cator, and H. Don. Random walks on \mathbb{Z} with metastable gaussian distribution caused by linear drift with application to the contact process on the complete graph, 2023.
- [4] Shankar Bhamidi, Danny Nam, Oanh Nguyen, and Allan Sly. Survival and extinction of epidemics on random graphs with general degree. *Ann. Probab.*, 49(1):244–286, 2021.
- [5] Béla Bollobás. *Random graphs*. Academic Press, Inc. [Harcourt Brace Jovanovich, Publishers], London, 1985.
- [6] E. Cator and H. Don. Explicit bounds for critical infection rates and expected extinction times of the contact process on finite random graphs. *Bernoulli*, 27(3):1556–1582, 2021.
- [7] E. Cator and P. Van Mieghem. Second-order mean-field susceptible-infected-susceptible epidemic threshold. *Phys. Rev. E*, 85:056111, May 2012.
- [8] E. Cator and P. Van Mieghem. Susceptible-infected-susceptible epidemics on the complete graph and the star graph: Exact analysis. *Phys. Rev. E*, 87:012811, Jan 2013.

- [9] E. Cator and P. Van Mieghem. Nodal infection in markovian susceptible-infected-susceptible and susceptible-infected-removed epidemics on networks are non-negatively correlated. *Phys. Rev. E*, 89:052802, May 2014.
- [10] Odo Diekmann, Hans Heesterbeek, and Tom Britton. *Mathematical tools for understanding infectious disease dynamics*. Princeton Series in Theoretical and Computational Biology. Princeton University Press, Princeton, NJ, 2013.
- [11] Peter Donnelly. The correlation structure of epidemic models. *Mathematical Biosciences*, 117(1):49–75, 1993.
- [12] Richard Durrett and Xiu Fang Liu. The contact process on a finite set. *Ann. Probab.*, 16(3):1158–1173, 1988.
- [13] P. Erdős and A. Rényi. On random graphs. I. *Publ. Math. Debrecen*, 6:290–297, 1959.
- [14] P. Erdős and A. Rényi. On the evolution of random graphs. *Magyar Tud. Akad. Mat. Kutató Int. Közl.*, 5:17–61, 1960.
- [15] A. Ganesh, L. Massoulié, and D. Towsley. The effect of network topology on the spread of epidemics. In *Proceedings IEEE 24th Annual Joint Conference of the IEEE Computer and Communications Societies.*, volume 2, pages 1455–1466 vol. 2, 2005.
- [16] E. N. Gilbert. Random graphs. *Ann. Math. Statist.*, 30:1141–1144, 1959.
- [17] James P. Gleeson. High-accuracy approximation of binary-state dynamics on networks. *Phys. Rev. Lett.*, 107:068701, Aug 2011.
- [18] T. E. Harris. Contact interactions on a lattice. *Ann. Probability*, 2:969–988, 1974.
- [19] Zhidong He and Piet Van Mieghem. The spreading time in sis epidemics on networks. *Physica A: Statistical Mechanics and its Applications*, 494:317–330, 2018.
- [20] Xiangying Huang and Rick Durrett. The contact process on random graphs and Galton Watson trees. *ALEA Lat. Am. J. Probab. Math. Stat.*, 17(1):159–182, 2020.
- [21] J.O. Kephart and S.R. White. Directed-graph epidemiological models of computer viruses. In *Proceedings. 1991 IEEE Computer Society Symposium on Research in Security and Privacy*, pages 343–359, 1991.
- [22] István Z Kiss, Joel C Miller, Péter L Simon, et al. Mathematics of epidemics on networks. *Cham: Springer*, 598(2017):31, 2017.
- [23] Thomas M. Liggett. Multiple transition points for the contact process on the binary tree. *Ann. Probab.*, 24(4):1675–1710, 1996.
- [24] Thomas M. Liggett. *Stochastic interacting systems: contact, voter and exclusion processes*, volume 324 of *Grundlehren der mathematischen Wissenschaften [Fundamental Principles of Mathematical Sciences]*. Springer-Verlag, Berlin, 1999.
- [25] David Machado and Roberto Mulet. From random point processes to hierarchical cavity master equations for stochastic dynamics of disordered systems in random graphs: Ising models and epidemics. *Physical Review E*, 104(5):054303, 2021.
- [26] Angélica S Mata and Silvio C Ferreira. Pair quenched mean-field theory for the susceptible-infected-susceptible model on complex networks. *Europhysics Letters*, 103(4):48003, 2013.
- [27] Cristopher Moore and M. E. J. Newman. Epidemics and percolation in small-world networks. *Phys. Rev. E*, 61:5678–5682, May 2000.

- [28] T. S. Mountford. A metastable result for the finite multidimensional contact process. *Canad. Math. Bull.*, 36(2):216–226, 1993.
- [29] Thomas Mountford, Daniel Valesin, and Qiang Yao. Metastable densities for the contact process on power law random graphs. *Electron. J. Probab.*, 18:No. 103, 36, 2013.
- [30] Jean-Christophe Mourrat and Daniel Valesin. Phase transition of the contact process on random regular graphs. *Electron. J. Probab.*, 21:Paper No. 31, 17, 2016.
- [31] Mark Newman. *Networks*. Oxford university press, 2018.
- [32] World Health Organization. *From emergency response to long-term COVID-19 disease management: sustaining gains made during the COVID-19 pandemic*, volume WHO/WHE/SPP/2023.1. WHO Geneva, 2023.
- [33] Ernesto Ortega, David Machado, and Alejandro Lage-Castellanos. Dynamics of epidemics from cavity master equations: Susceptible-infectious-susceptible models. *Physical Review E*, 105(2):024308, 2022.
- [34] Romualdo Pastor-Satorras, Claudio Castellano, Piet Van Mieghem, and Alessandro Vespignani. Epidemic processes in complex networks. *Rev. Modern Phys.*, 87(3):925–979, 2015.
- [35] Romualdo Pastor-Satorras and Alessandro Vespignani. Epidemic dynamics and endemic states in complex networks [j]. *Physical review. E, Statistical, nonlinear, and soft matter physics*, 63:066117, 07 2001.
- [36] Robin Pemantle. The contact process on trees. *Ann. Probab.*, 20(4):2089–2116, 1992.
- [37] Diogo H Silva, Silvio C Ferreira, Wesley Cota, Romualdo Pastor-Satorras, and Claudio Castellano. Spectral properties and the accuracy of mean-field approaches for epidemics on correlated power-law networks. *Physical Review Research*, 1(3):033024, 2019.
- [38] Diogo H Silva, Francisco A Rodrigues, and Silvio C Ferreira. High prevalence regimes in the pair-quenched mean-field theory for the susceptible-infected-susceptible model on networks. *Physical Review E*, 102(1):012313, 2020.
- [39] Alan Stacey. The contact process on finite homogeneous trees. *Probab. Theory Related Fields*, 121(4):551–576, 2001.
- [40] Ruud van de Bovenkamp and Piet Van Mieghem. Survival time of the susceptible-infected-susceptible infection process on a graph. *Physical Review E*, 92(3):032806, 2015.
- [41] Remco van der Hofstad. *Random graphs and complex networks. Vol. 1*, volume [43] of *Cambridge Series in Statistical and Probabilistic Mathematics*. Cambridge University Press, Cambridge, 2017.
- [42] Piet Van Mieghem. The n-intertwined sis epidemic network model. *Computing*, 93(2):147–169, 2011.
- [43] Piet Van Mieghem, Jasmina Omic, and Robert Kooij. Virus spread in networks. *IEEE/ACM Transactions on Networking*, 17(1):1–14, 2009.
- [44] Yang Wang, D. Chakrabarti, Chenxi Wang, and C. Faloutsos. Epidemic spreading in real networks: an eigenvalue viewpoint. In *22nd International Symposium on Reliable Distributed Systems, 2003. Proceedings.*, pages 25–34, 2003.